

Hrvatski meteorološki časopis, 39, 15–39, 2004.

UDK: 551.509.333  
Izvorni znanstveni rad

## SEASONAL DYNAMICAL DOWNSCALING WITH ERA-40 DATA: A SENSITIVITY STUDY

### Sezonska dinamička prilagodba ERA-40 podataka: studija osjetljivosti

ČEDO BRANKOVIĆ, MIRTA PATARČIĆ and LIDIJA SRNEC

Croatian Meteorological and Hydrological Service  
Grič 3, 10000 Zagreb, Croatia  
brankovic@cirus.dhz.hr  
patarcic@cirus.dhz.hr  
srnec@cirus.dhz.hr

*Primljeno 15. siječnja 2005., u konačnom obliku 4. veljače 2005.*

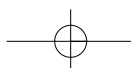
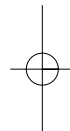
**Abstract:** The Regional Climate Model (RegCM) with 50 km horizontal resolution was used for seasonal dynamical downscaling of ECMWF ERA-40 data over central and southern Europe and the northern Mediterranean region for one winter and one summer season. Various configurations in initial conditions (ICs) and lateral boundary conditions (LBCs) as well as in the model vertical domain were tested. First, the horizontal resolution of ICs and LBCs was increased from T42 to T159 and then a gradual “degradation” was conducted: the frequency of the LBCs update was reduced from 6-hourly to 12-hourly intervals, the model top was lowered from 100 to 200 hPa and the number of vertical levels was reduced from 18 to 14. The latest, most “degraded”, configuration is the closest to that available in the ECMWF seasonal forecast archive.

The limited number of experiments (a single experiment per configuration and per season) did not allow a thorough statistical assessment of model responses; however, it can be concluded that, though the differences between various configurations and resolutions are generally small, they are far from being negligible. The increase in the ICs and LBCs horizontal resolution yields a reduction in geopotential, in both the upper-air and surface temperature (cooling) and a reduction in the summer convective precipitation. The reduced, 12-hourly, frequency of the LBCs update mostly renders the opposite result, i.e. an increase in geopotential and temperature. However, it was not possible to fully establish how actually detrimental this reduced frequency in LBCs is, because the input ERA-40 upper-air data “oscillate” between consecutive 6 hours due to the difference in the processing of temperatures from satellites and from radiosondes within the ECMWF 3D-Var assimilation system.

The model upper troposphere winds are strengthened when the model top is lowered; however, this effect is partly offset when the number of model levels is reduced. Changes in the model vertical configuration cause on average much weaker effects on surface fields than changes in LBCs. The Arakawa-Schubert closure in the parameterisation of convection reduces the amount of summer convective precipitation over the northern European lowlands when compared with the Fritsch-Chappel closure. However, in a large portion of the integration domain precipitation is still too high in respect of the CRU observational data.

**Key words:** dynamical downscaling, RegCM, ERA-40

**Sažetak:** Regionalni klimatski model (RegCM), s horizontalnom rezolucijom od 50 km, korišten je za dinamičku prilagodbu (*downscaling*) ERA-40 sezonskih podataka ECMWF-a za područje središnje i južne Europe i sjevernog dijela Sredozemlja u jednoj zimskoj i ljetnoj sezoni. Ispitane su različite konfiguracije početnih i rubnih uvjeta kao i vertikalne domene modela. Najprije je povećana horizontalna rezolucija početnih i rubnih uvjeta s T42 na T159, a zatim je provedena njihova postupna “degradacija”: frekvencija učitavanja rubnih uvjeta smanjena je sa 6-satnih na 12-satne intervale, gornja granica modela spuštena je sa 100 na 200 hPa i broj vertikalnih nivoa smanjen je s 18 na 14. Ta zadnja, “najlošija” konfiguracija modela najslabija je konfiguraciji sezonskih



prognoza iz arhive ECMWF-a.

Ograničen broj eksperimenata (jedan eksperiment po konfiguraciji i po sezoni) ne omogućuje temeljitu statističku procjenu uspješnosti modela; ipak, može se zaključiti da se razlike između različitih konfiguracija i rezolucija, iako općenito male, ne mogu zanemariti. Povećanje horizontalne rezolucije početnih i rubnih uvjeta uzrokuje smanjenje geopotencijala, prizemne temperature i temperature u visini (hlađenje) i smanjenje ljetne konvektivne oborine. Reducirana, 12-satna frekvencija rubnih uvjeta uglavnom daje suprotne rezultate, tj. povećanje geopotencijala i temperature. Međutim, nije bilo moguće u potpunosti odrediti štetan učinak smanjene frekvencije rubnih uvjeta jer ulazni visinski ERA-40 podaci "osciliraju" između uzastopnih 6-satnih termina zbog razlika u obradi temperaturnog polja između satelitskih i radiosondažnih podataka unutar 3D-Var asimilacijskog sustava ECMWF-a.

Spuštanje vrha modela uzrokuje pojačanje vjetra u gornjoj troposferi modela; međutim, taj efekt djelomice je poništen smanjenjem broja nivoa u modelu. Promjene u vertikalnoj konfiguraciji modela uzrokuju u prosjeku mnogo slabije efekte na prizemna polja nego promjene rubnih graničnih uvjeta. Arakawa-Shubertovo zatvaranje u usporedbi s Fritsch-Chappelovim zatvaranjem u parametrizaciji konvekcije smanjuje ljetnu konvektivnu oborinu iznad nizinskog dijela sjeverne Europe. Ipak, u većem dijelu područja integracije oborina je još uvijek prevelika u odnosu na CRU podatke mjerenja.

**Ključne riječi:** dinamička prilagodba (*downscaling*), RegCM, ERA-40

## 1. INTRODUCTION

The usefulness of general circulation models (GCMs) for studying climate and climate variability on smaller or local scales is rather limited because of their relative coarse resolutions. Even with continuous improvements in the horizontal resolution of climate GCMs there will be a need to downscale the model output to smaller scales for the purpose of impact studies or comparisons with station data. Often only downscaled results are good enough for further application in, for example, hydrological models and crop-yield models or for air pollution studies. These applications are becoming increasingly important in studies of the local effects of climate change.

The dynamical downscaling or downscaling by using limited-area climate models is one of the four downscaling techniques classified by Wilby and Wigley (1997). The other three include regression methods, weather pattern approaches and stochastic weather generators. Though perhaps most physically justifiable, the main shortcoming of dynamical downscaling is its almost complete dependence on the quality of GCM products. Every model contains errors of some sort and one of the main causes of errors, even at spatial resolutions of limited-area models, is the inadequate representation of orography. Irrespective of this potential problem of representing small-scale orographic features, Zeng and Pielke (1995) have shown that various physical quantities,

like sensible heat, moisture and momentum fluxes, can have a different amplitude and vertical structure in limited area climate models than those typical of a GCM grid box.

Within the climate modelling community, the Regional Climate Model (RegCM) is one of the most frequently and widely used models for dynamical downscaling. It has been used for studying various aspects of the Earth climate, from short-term regional climate variability to long climate simulations that involve climate scenarios with natural and anthropogenic changes. It has been used and tested over various regions and with various configurations, parameterisation schemes and types of forcing. A large body of literature on the RegCM is given in, for example, Giorgi and Mearns (1999).

One of the main objectives for employing the RegCM at the Croatian Meteorological and Hydrological Service (CMHS) is to dynamically downscale the operational seasonal forecasts of the European Centre for Medium-Range Weather Forecasts (ECMWF). However, this is not a straightforward task since the ECMWF seasonal data archive contains only a limited amount of meteorological parameters available at a limited time frequency and at a restricted number of pressure levels. These constraints may pose a serious difficulty to the whole process of downscaling and eventually make it impracticable. It was therefore necessary to assess the sensitivity of the

RegCM to degrading forcing imposed by initial conditions (ICs) and lateral boundary conditions (LBCs). Such a testing was made possible by using the ECMWF re-analysis data, ERA-40 – the dataset that contains a relative large number of physical fields at a relatively high temporal frequency and defined at more vertical levels when compared with the ECMWF seasonal forecasts archive. The testing was performed in such a way that the RegCM was run with various configurations defined by gradually reducing the availability of ICs and LBCs to eventually match those of seasonal forecasts.

Throughout the paper, we focus on seasonally averaged quantities. Neither monthly means nor intraseasonal variability were studied here, though by virtue of experiment design that would be possible. Our prime interest lies in the seasonally downscaled averages so as to be able to eventually make comparisons with the ECMWF seasonal operational products that are produced by the ECMWF GCM.

In the next section, a brief description of the RegCM used in this study together with an explanation of the experiments is given. In section 3 we assess the impact of various configurations in ICs, LBCs and in the model. The emphasis is on the former, because in order to carry out a downscaling of the ECMWF operational seasonal forecasts one has to reconcile with the availability of the ECMWF seasonal forecast archive. Section 4 deals with the impacts of the two different closures in the convection scheme that have been tested in our summer integrations. In section 5, a basic verification of some model results is presented, and in section 6 the summary and conclusions are given.

## 2. MODEL AND EXPERIMENTS

### 2.1. The RegCM

The model used for this study was the so-called RegCM3, the third-generation RegCM that draws from early work by Dickinson et al. (1989) and Giorgi (1990). It was built upon the National Center for Atmospheric Research (NCAR) and Pennsylvania State University (PSU) mesoscale model, MM4. The first major upgrade of the original RegCM numerics and physics (RegCM2) is documented in Giorgi et al. (1993 a,b).

The RegCM is defined in the  $\sigma$  vertical coordinate system – model levels close to the earth's surface follow the terrain, the levels higher up coincide with pressure levels. The model dynamics and numerics are given in Grell et al. (1994). The radiation scheme has been taken from the NCAR CCM3 model (Kiehl et al., 1996). The land surface model is the so-called Biosphere-Atmosphere Transfer Scheme (BATS) described in Dickinson et al. (1993) and the planetary boundary layer (PBL) scheme was developed by Holtslag et al. (1990). There is a choice of convection parameterisations between the Grell scheme (Grell, 1993), the modified Kuo scheme (Anthes, 1977) and the Betts-Miller scheme (Betts and Miller, 1993). The Grell convection offers two alternative closures: the Fritsch-Chappel closure (Fritsch and Chappel, 1980) and the Arakawa-Schubert closure (Arakawa and Schubert, 1974). Large-scale precipitation is parameterised by the Sub-grid Explicit Moisture Scheme (SUBEX, Pal et al., 2000). There are two options for the ocean flux parameterisation – the BATS and the Zeng scheme (Zeng et al., 1998).

In our experiments, the horizontal resolution used was 50 km in the area of 60x50 grid points centred at 45°N, 16°E, thus covering central and southern Europe and the northern Mediterranean. The model domain may seem rather small compared to some other studies with the RegCM (e.g. Giorgi et al., 2004), however, it was primarily constrained by available computer resources. It would be desirable, for example, to extend the western boundary further west to allow the Atlantic synoptic systems to better develop into the model domain and to place it further away from the major topographic features, like the Alps, the Atlas Mountains and the Pyrenees. In the control experiment, the number of levels in the vertical was 18, extending from the surface to 100 hPa. The Lambert conformal projection, suitable for mid-latitudes was used. For the convection, the Grell scheme was chosen with both Fritsch-Chappel and Arakawa-Schubert closures tested.

### 2.2. Definition of lateral boundary conditions (LBCs) and experimental design

In all the experiments described and discussed in this paper, the ICs and LBCs were taken from the ECMWF re-analysis, ERA-40. The

following fields were retrieved from the ERA-40 archive: surface pressure, geopotential height, temperature, u and v wind components and specific humidity. The upper-air fields were defined at standard pressure levels, from 1000 to 100 hPa. Then, the ERA-40 data were converted from the original Grib format to the one suitable for the RegCM.

Over the oceans, the model was forced by the observed sea surface temperatures (SSTs) obtained from the National Ocean and Atmosphere Administration (NOAA). These were derived by an optimal interpolation procedure from weekly analyses on a regular 1x1 deg latitude/longitude grid.

The originally available ERA-40 data for the RegCM forcing (obtained from the Abdus Salam International Centre for Theoretical Physics (ICTP), Trieste, Italy) were at a lower horizontal resolution (T42) than found in the ECMWF ERA-40 archive (T159). These low resolution LBCs (and ICs), denoted as LR in Table 1, were available at a 6-hour time frequency, denoted as F6. Thus, LR\_F6 is considered to be the control experiment (see Table 1). As mentioned above, it was run with 18 levels in the vertical with the top of the model at 100 hPa. No other experiment was forced with the T42 data. In all model runs, both the ICs and LBCs were, of course, interpolated to the model grid described in the previous subsection and to model  $\sigma$  levels.

Table 1. Definition of experiments in dynamical seasonal downscaling. The experiments are named according to the horizontal resolution of ICs and LBCs (LR and HR respectively), the frequency of LBC updating (F6 and F12), the number of levels in the vertical, the top level in the model and the closure scheme for the parametrization of convection.

Tablica 1. Eksperimenti dinamičke sezone prilagodbe (*downscalinga*). Eksperimenti su nazvani prema horizontalnoj rezoluciji početnih i rubnih uvjeta (LR odnosno HR), frekvenciji učitavanja rubnih uvjeta (F6 i F12), broju vertikalnih nivoa, visini najvišeg nivoa u modelu i shemi zatvaranja konvektivne parametrizacije.

Experiment name	IC and LBC resolution	LBC frequency	Number of levels	Model top (mb)	Closure for convection	
					JJA	DJF
LR_F6	T42	6-hourly	18	100	FC	FC
HR_F6	T159	6-hourly	18	100	FC, AS	FC
HR_F12	T159	12-hourly	18	100	FC, AS	FC
HR_T200	T159	12-hourly	18	200	AS	FC
HR_L14	T159	12-hourly	14	200	AS	FC

LR - low resolution (niska rezolucija)

HR - high resolution (visoka rezolucija)

F6 - 6-hourly update of LBCs (6-satno učitavanje rubnih uvjeta)

F12 - 12-hourly update of LBCs (12-satno učitavanje rubnih uvjeta)

FC - Fritsch-Chappel closure (Fritsch-Chappelovo zatvaranje)

AS - Arakawa-Schubert closure (Arakawa-Schubertovo zatvaranje)

A configuration identical to that for T42 was applied to a higher horizontal resolution, T159 (denoted as HR in Table 1), thus making the HR\_F6 experiment. The comparison of the LR\_F6 and HR\_F6 experiments gives an estimate of the impact of horizontal resolution in the initial and boundary conditions on model integrations.

The next step was to reduce the frequency of LBCs from 6-hourly to 12-hourly intervals. This was done only for the T159 LBCs (therefore HR\_F12 in Table 1). The comparison of HR\_F6 and HR\_F12 is crucial since in the latter the RegCM might be deprived of some important data at the boundary required to better define, for example, diurnal cycle. The 12-hourly frequency of updating model LBCs was retained in the next two experiments. In the first, the top of the model was lowered from the original 100 hPa to 200 hPa, and in the second, the number of the model vertical levels was reduced from the original 18 to 14 (hence in Table 1 HR\_T200 and HR\_L14, respectively). With these two last modifications the model and the LBCs configurations were brought close to that of the ECMWF seasonal forecast archive.

Finally, test runs were done on the impact of the two different closures for the modelled convection scheme, i.e. the Fritsch-Chappel closure was compared with the Arakawa-Schubert one. This comparison was carried

out for summer integrations only and not for all the model and LBCs configurations (see Table 1).

The usual length of our model integrations was a little longer than three months. For diagnostic and verification purposes two different seasons were considered: December to February (DJF) 1993/94 and June to August (JJA) 1997.

### 3. IMPACT OF VARIOUS CONFIGURATIONS ON SEASONAL DOWNSCALING

The rather limited number of experiments carried out make it almost impossible to confidently attach statistical significance to our results. Nevertheless, many of the differences between the various model/LBCs configurations considered are not negligible and are consistent for, say, different seasons or for different convection closures. Therefore, we may assume that the differences in the results from

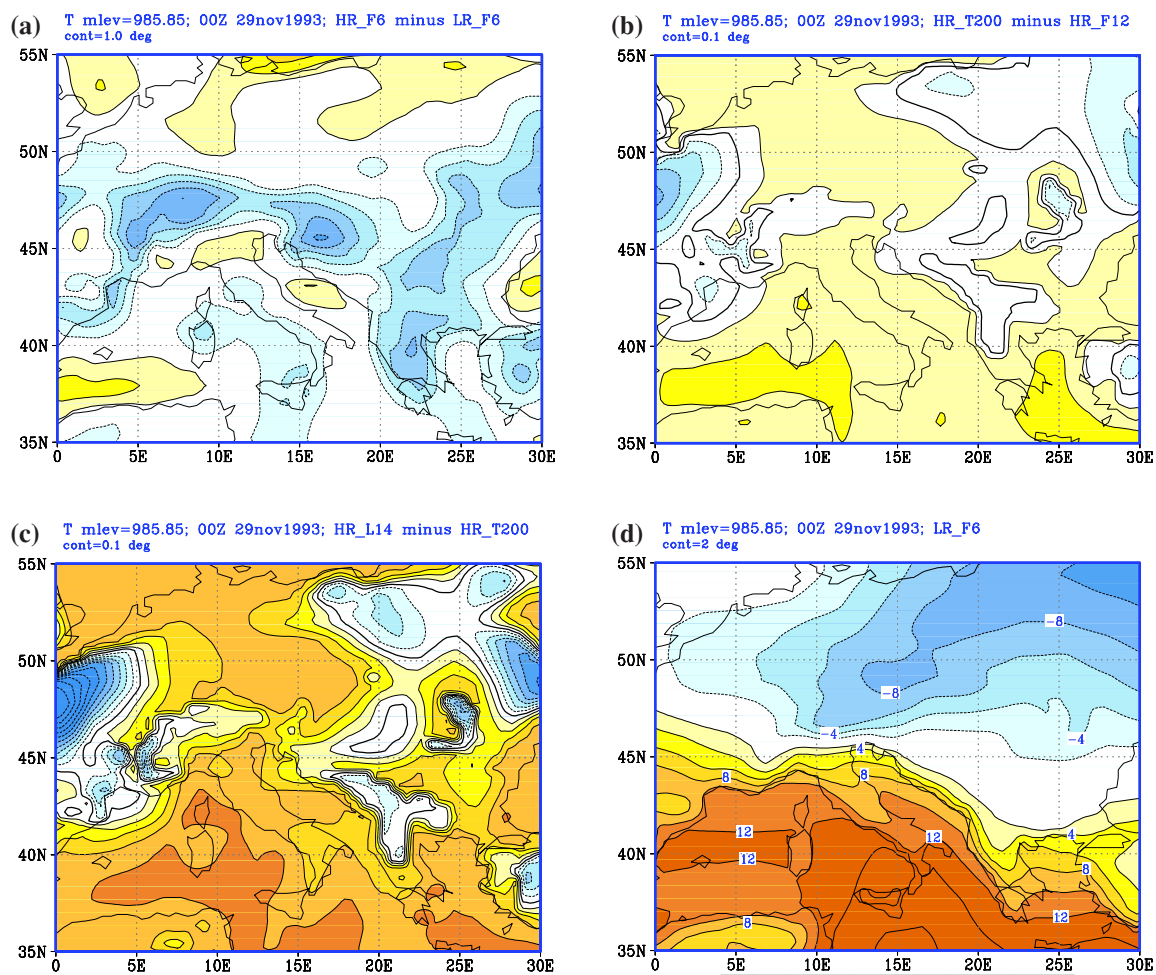


Figure 1. Initial temperature at model level corresponding to 985 hPa for 00Z 29 November 1993. Differences for (a) HR\_F6 minus LR\_F6, (b) HR\_T200 minus HR\_F12, (c) HR\_L14 minus HR\_T200 and (d) full field for the control experiment LR\_F6. Contours for differences in (a) every 1 deg, in (b) and (c) every 0.1 deg and for the full field in (d) every 2 deg.

Slika 1. Početna temperatura na nivou modela blizu 985 hPa u 00UTC 29. studenog 1993. Razlike (a) HR\_F6 minus LR\_F6, (b) HR\_T200 minus HR\_F12, (c) HR\_L14 minus HR\_T200 i (d) puno temperaturno polje u kontrolnom eksperimentu LR\_F6. Izolinije razlika u (a) svakih 1°, u (b) i (c) svakih 0.1° i za puno polje u (d) svaka 2°.

one configuration to another reflect the true impact of the imposed changes. The organisation of this section runs according to the changes introduced to the ICs, LBCs and model configurations.

### 3.1. Differences in ICs

We first discuss the differences in ICs for various configurations as described in Table 1. The ICs would primarily have an impact on initial model results and during the early stage of model runs. The overall impact on, say, seasonal averages is determined primarily by LBCs and in the interior of the integration domain by the model physics and dynamics. Therefore, we only illustrate the differences in the ICs for a given model initial time – in this particular case we have chosen the initial time of our winter integrations, 29 November 1993 at 00Z.

From Figure 1 it is clear that the largest differences in the ICs appear when the horizontal resolution of the input data is changed from T42 to T159 (HR\_F6 minus LR\_F6, Fig. 1(a); note the different contouring intervals in Figure 1 (a) to (c)). The temperature differences at model  $\sigma$  level that corresponds to approximately 985 hPa indicate a relatively strong cooling in the central and eastern parts of the integration domain, reaching 5 deg over central Croatia. This cooling increases the initial temperature gradient (and consequently low-level winds) to the south of the Alps in the HR\_F6 experiment with respect to the control experiment LR\_F6 (Fig. 1(d)). When the model top is lowered from 100 to 200 hPa (Fig. 1 (b)) and when the number of model levels is reduced from 18 to 14 (Fig. 1 (c)), the temperature differences are much smaller than those when the horizontal resolution of initial data was changed. In addition, the prevailing sign of the differences in Figure 1 (b) and (c) is opposite to the one that dominates in Figure 1(a), i.e. the changes in the model vertical structure are causing a warming at low levels in a large portion of the integration domain. (In the above consideration, the change of the LBCs frequency update i.e. the difference HR\_F12 minus HR\_F6 has no relevance for a possible impact on the ICs.)

The same pattern of differences as described above applies to many other multi-level fields (e.g. wind, humidity). The notable exception is temperature at the  $\sigma$  level(s) close to the model

top – when the model top is lowered, temperature experiences a change comparable to that when the horizontal resolution was increased (not shown). These results indicate how simple changes in either horizontal or vertical resolution can generate different initial conditions though they start from seemingly identical fields. These initial differences might eventually lead to different model responses; however, as mentioned above, at later stages in the model run, the model LBCs take over and make a decisive impact on model development.

### 3.2. High versus low resolution LBCs

In contrast to the changes in ICs, the changes to the LBCs' configurations have a continuous impact on the model integrations. Therefore, in this and the following subsections, the results of seasonal downscaling are discussed in terms of seasonal averages for the various experiments from Table 1.

Before focusing on model results, we briefly comment (without showing figures) the difference between the T159 (HR\_F6) and T42 (LR\_F6) resolutions in the ERA-40 input data. This is essential, because some of the differences between the HR\_F6 and LR\_F6 experiments shown in subsections (a) and (b) below might be linked to or might originate from the differences in the data that were used to force our model integrations. For this purpose we compared the T42 and T159 ERA-40 data – interpolated to the model levels and model grid, and averaged for both DJF and JJA.

Irrespective of season, the T159 minus T42 difference yields a reduction in temperature (cooling) throughout the model atmosphere. This cooling is generally stronger in DJF than in JJA. In the lower troposphere the cooling is, on average, twice as large as in the middle or upper troposphere. For example, at model level close to 850 hPa, in the northeastern parts of the model domain, the DJF cooling exceeds -1.2 deg, whereas at model level close to 300 hPa this is about -0.5 deg over central Europe and the southern Balkan Peninsula. At model low levels, cooling in T159 is associated with drying, exceeding locally 2.0 gkg<sup>-1</sup> during the JJA season; however, over some relatively small areas some moistening is observed as well. In contrast to the temperature change, drying is more pronounced in JJA than in DJF.

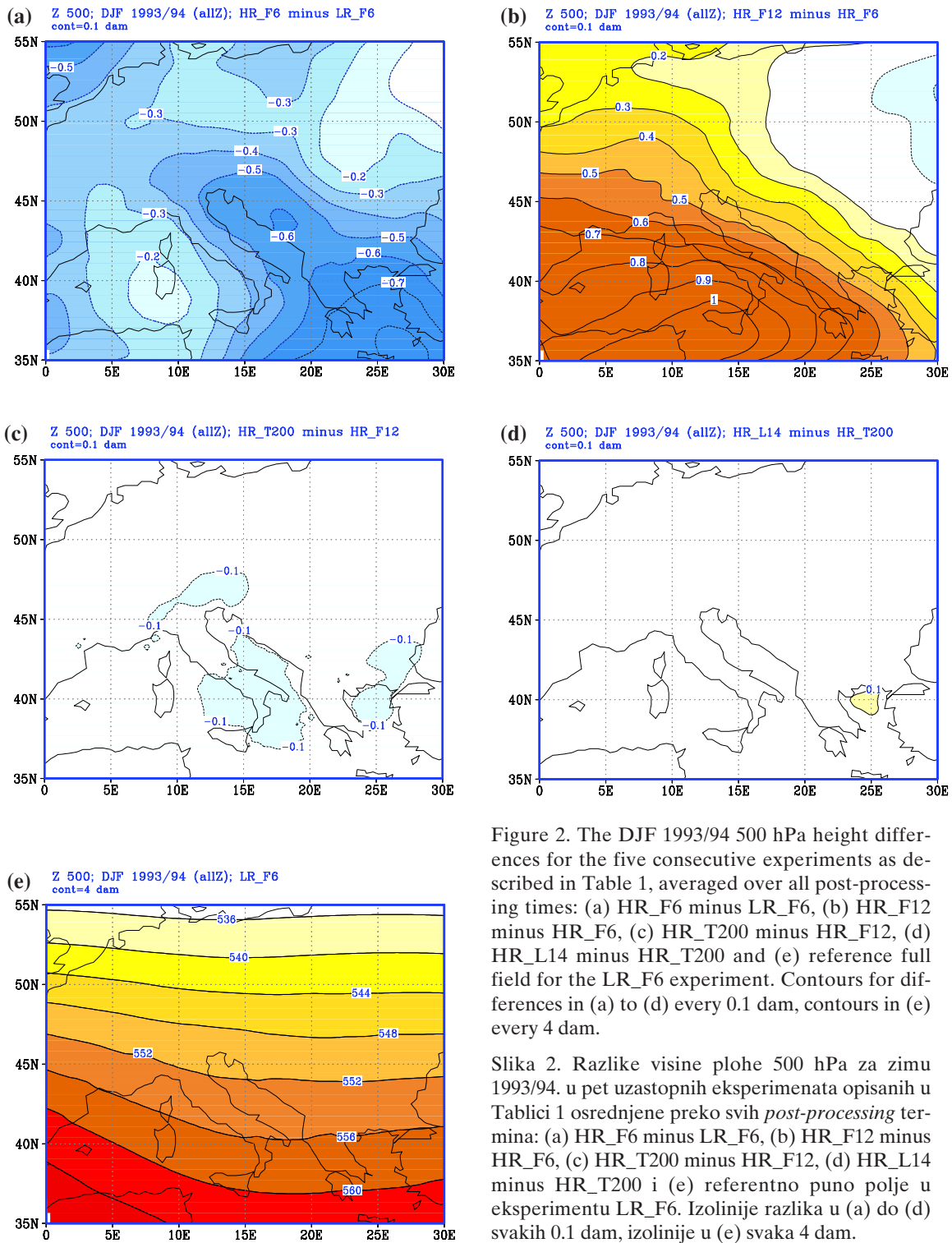


Figure 2. The DJF 1993/94 500 hPa height differences for the five consecutive experiments as described in Table 1, averaged over all post-processing times: (a) HR\_F6 minus LR\_F6, (b) HR\_F12 minus HR\_F6, (c) HR\_T200 minus HR\_F12, (d) HR\_L14 minus HR\_T200 and (e) reference full field for the LR\_F6 experiment. Contours for differences in (a) to (d) every 0.1 dam, contours in (e) every 4 dam.

Slika 2. Razlike visine plohe 500 hPa za zimu 1993/94. u pet uzastopnih eksperimenata opisanih u Tablici 1 osrednjene preko svih *post-processing* termina: (a) HR\_F6 minus LR\_F6, (b) HR\_F12 minus HR\_F6, (c) HR\_T200 minus HR\_F12, (d) HR\_L14 minus HR\_T200 i (e) referentno puno polje u eksperimentu LR\_F6. Izolinije razlika u (a) do (d) svakih 0.1 dam, izolinije u (e) svaka 4 dam.

In accordance with the DJF cooling described above, low-level winds from western into central Europe as well as over the western Mediterranean are stronger at T159 than at T42, with an amplitude exceeding  $2.5 \text{ ms}^{-1}$  on the windward side of the Alps. Similarly, the northern Mediterranean summer north-westerlies are stronger at T159 than at T42. However, over the eastern Mediterranean and Turkey they are weakened by approximately the same amount.

Some of the differences between the ERA-40 T159 and T42 data discussed above are brought into the model integrations, primarily through the forcing at lateral boundaries. However, it is difficult to quantify and to fully separate such an impact from the “pure” model impact. Hence, the model results discussed throughout the rest of this subsection must be also viewed in relation to the differences between the two horizontal resolutions in the input ERA-40 data.

#### (a) Upper-air fields

Figure 2 (a) shows the mean DJF difference in the 500 hPa geopotential heights between the HR\_F6 and LR\_F6 experiments over central Europe and the northern Mediterranean region. The averaging is made over all post-processing times (four times a day at 00, 06, 12 and 18Z). The overall impact of the increased resolution in LBCs is a reduction in the 500 hPa geopotential height. This is more pronounced in the central (Adriatic) and south-eastern part of the integration domain, where the maximum difference reaches more than 0.8 dam. The differences refer to the deepening of the (seasonally averaged) trough in the Mediterranean region (c.f. Fig. 2(e)). A similar pattern, a reduction in geopotential heights, emerges in the summer season as well, however, with a somewhat reduced amplitude of differences (not shown).

The vertical structure of the differences in the region of interest is assessed from zonally averaged cross sections between  $12^{\circ}\text{E}$  and  $20^{\circ}\text{E}$  (Fig. 3). For the HR\_F6 minus LR\_F6 differences (Fig. 3, left panels), a reduction in geopotential height throughout the model atmosphere is seen. In winter, largest differences are found in the middle of the integration domain with an indication of increased differ-

ences at the northern and southern boundaries (Fig. 3 (a)). In summer, negative differences are larger in the Mediterranean region than in central Europe, as well as close to the model top, where they amount to over 0.8 dam (Fig. 3 (c)).

In contrast to geopotential height, the DJF negative temperature differences (cooling) between HR\_F6 and LR\_F6 are mainly confined to the lower part of the troposphere, below 700 hPa. Above this level, the temperature differences are neutral (not shown). In summer, the largest negative temperature differences are in the upper troposphere, similar to those for geopotential height. These results are broadly consistent with the discussion at the beginning of this subsection on the differences between seasonally averaged ERA-40 data for the two resolutions considered.

In the above figures, the averaging over all post-processing times flattens out the diurnal cycle. Although it may be argued that the diurnal cycle for some upper-air parameters (like geopotential or wind) is small anyway, its effect can be more pronounced for some other parameters or/and levels, especially if closer to the ground. Indeed, as shown in Figure 4 this is the case for the HR\_F6 minus LR\_F6 differences for the JJA 850 hPa temperature at 00Z and 12Z. Though the impact of the changed resolution in LBCs is rather similar in both mid-day and mid-night times, they clearly differ in some details. The differences are largest over the mountains: the Alps, the Dinaric Alps and the mountains of the southern Balkan, the Carpathian Mountains, the Pyrenees and the mountains of north Africa. For example, over the Alps, the day-time differences exceed by about 0.5 deg those during night-time. The differences are even larger over the mountains of the southern Balkan, reaching about 1 deg. At 18Z the differences are smaller than those at 12Z, but larger than that at 00Z (not shown). This may have some implications on the model results when the LBCs with reduced time frequency are used to force the model (see subsection 3.3).

#### (b) Surface fields

For the HR\_F6 minus LR\_F6 difference, the dominant feature in the DJF 1993/94 total precipitation is a reduction in the central part of

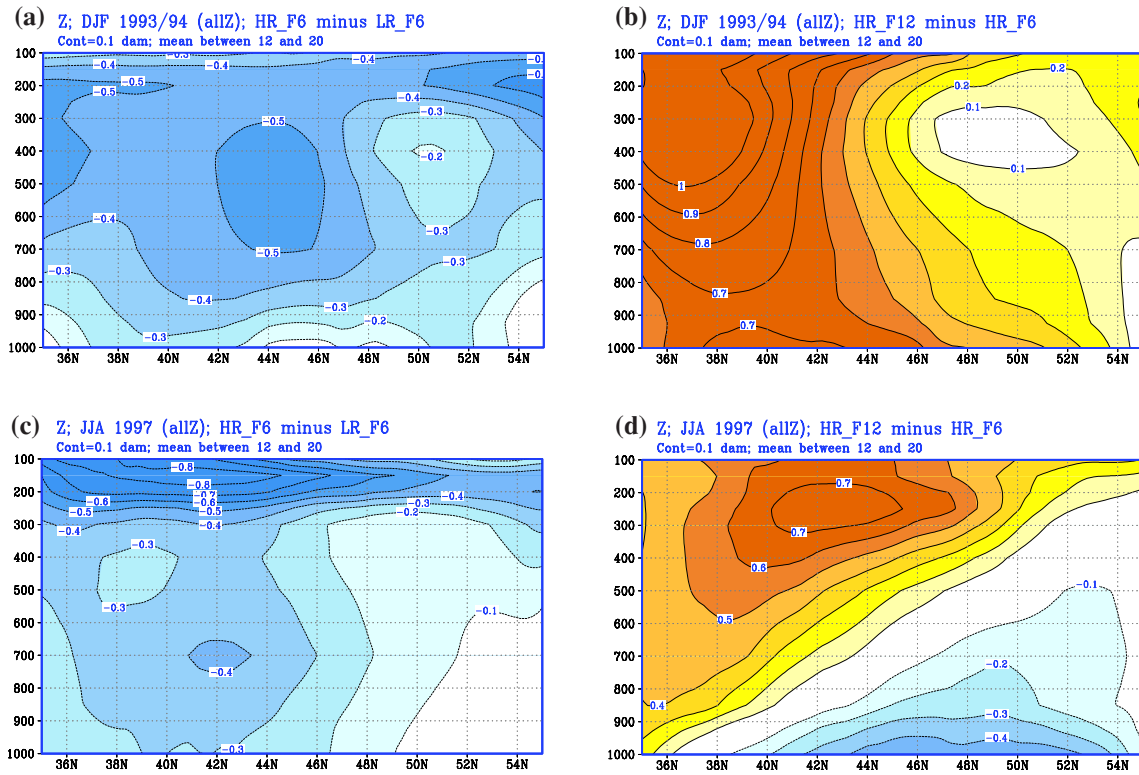
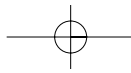


Figure 3. Zonally-averaged cross sections between 12°E and 20°E for the differences HR\_F6 minus LR\_F6 (left) and HR\_F12 minus HR\_F6 (right), for DJF 1993/94 (top) and JJA 1997 (bottom). Contours every 0.1 dam.

Slika 3. Zonalno osrednjeni vertikalni presjeci između 12°E i 20°E za razlike HR\_F6 minus LR\_F6 (lijevo) i HR\_F12 minus HR\_F6 (desno), za zimu 1993/94. (gore) i ljeto 1997. (dolje). Izolinije svakih 0.1 dam.

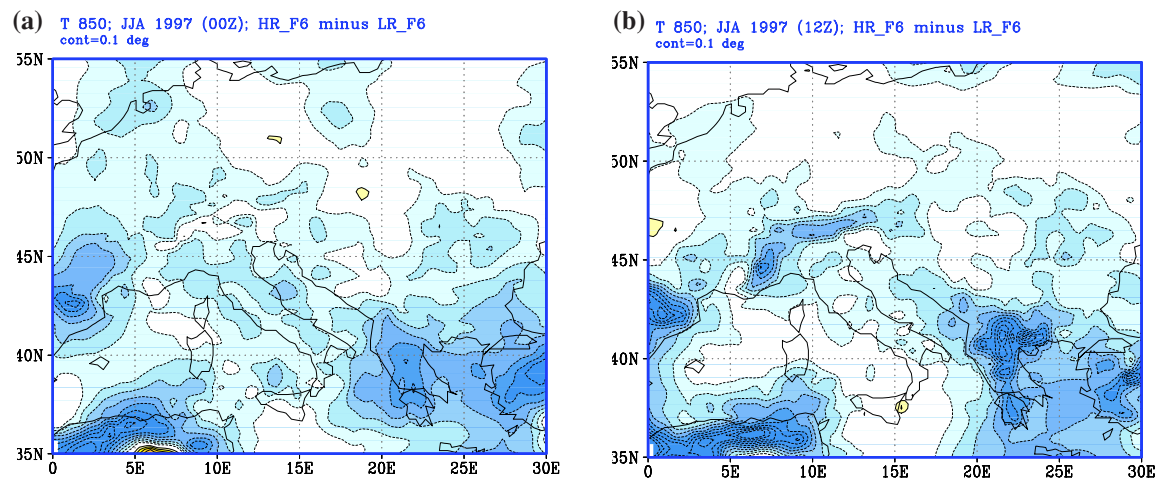
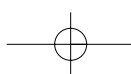


Figure 4. The JJA 1997 850 hPa temperature differences between the HR\_F6 and LR\_F6 experiments for (a) 00Z and (b) 12Z. Contours every 0.1 deg.

Slika 4. Razlike temperature u ljeto 1997. na plohi 850 hPa između eksperimenata HR\_F6 i LR\_F6 u (a) 00UTC i (b) 12UTC. Izolinije svakih 0.1°.



the integration domain and an increase in the surrounding area (Fig. 5 (a)). The negative-positive dipole in the precipitation differences over the eastern Adriatic coast indicates a strengthening of the southeast Europe precipitation maximum in HR\_F6 when compared to the control, LR\_F6 (Fig. 5(e)). The dipole trough-to-ridge amplitude is more than  $3 \text{ mm day}^{-1}$ . Generally, it is difficult to fully associate the differences in Fig. 5 (a) with the major mountain ranges in central and south Europe. For example, though in the Alpine region positive differences prevail, some negative differences in the eastern part are seen as well. Moreover, relatively large positive differences are found over the southeastern, Mediterranean, corner. This may be associated with the downstream shift of precipitation due to increased upper-air wind in this region in the HR\_F6 experiment (not shown). Pan et al. (1999) also reported such a shift of precipitation and attributed it to a long continuous integration of the RegCM2. Namely, when the model was frequently reinitialised such a shift did not occur or was much weaker.

For the JJA total precipitation, again, no prevailing or typical pattern is found for the HR\_F6 minus LR\_F6 differences (not shown). However, in convective precipitation negative differences (i.e. a reduction of convective precipitation in the higher resolution LBCs) clearly prevail over much of the land areas (Fig.6 (a)).

For the 12Z 2m temperature, the DJF 1993/94 differences between HR\_F6 and LR\_F6 are largely negative, reaching nearly 1 deg in the region to the north of the Alps and about 1.5 deg in the Hungarian plain (Fig. 7(a)). When compared with the DJF 1993/94 observational data from northern Croatia, where flat lowland terrain prevails, the 2m temperature in the control experiment, LR\_F6, is found to be too warm (Fig. 7(e)). Therefore, the apparent cooling in the HR\_F6 experiment seems to bring 2m temperature closer to reality. In contrast to precipitation, the 12Z summer 2m temperature differences between HR\_F6 and LR\_F6 could be linked to orographic features (not shown). Over many bordering mountains (like the Atlas Mountains in north Africa, the Pyrenees, the mountains of Greece and Turkey) a cooling of more than 2 deg is found. Clearly, in the bordering regions where model integration is mostly influenced by LBCs, the

higher the horizontal resolution the better the representation of the orographic influence in the HR\_L6 LBCs. Thus, the cooling of the bordering 2m temperature in the HR\_F6 (implicitly) indicates higher mountain elevations.

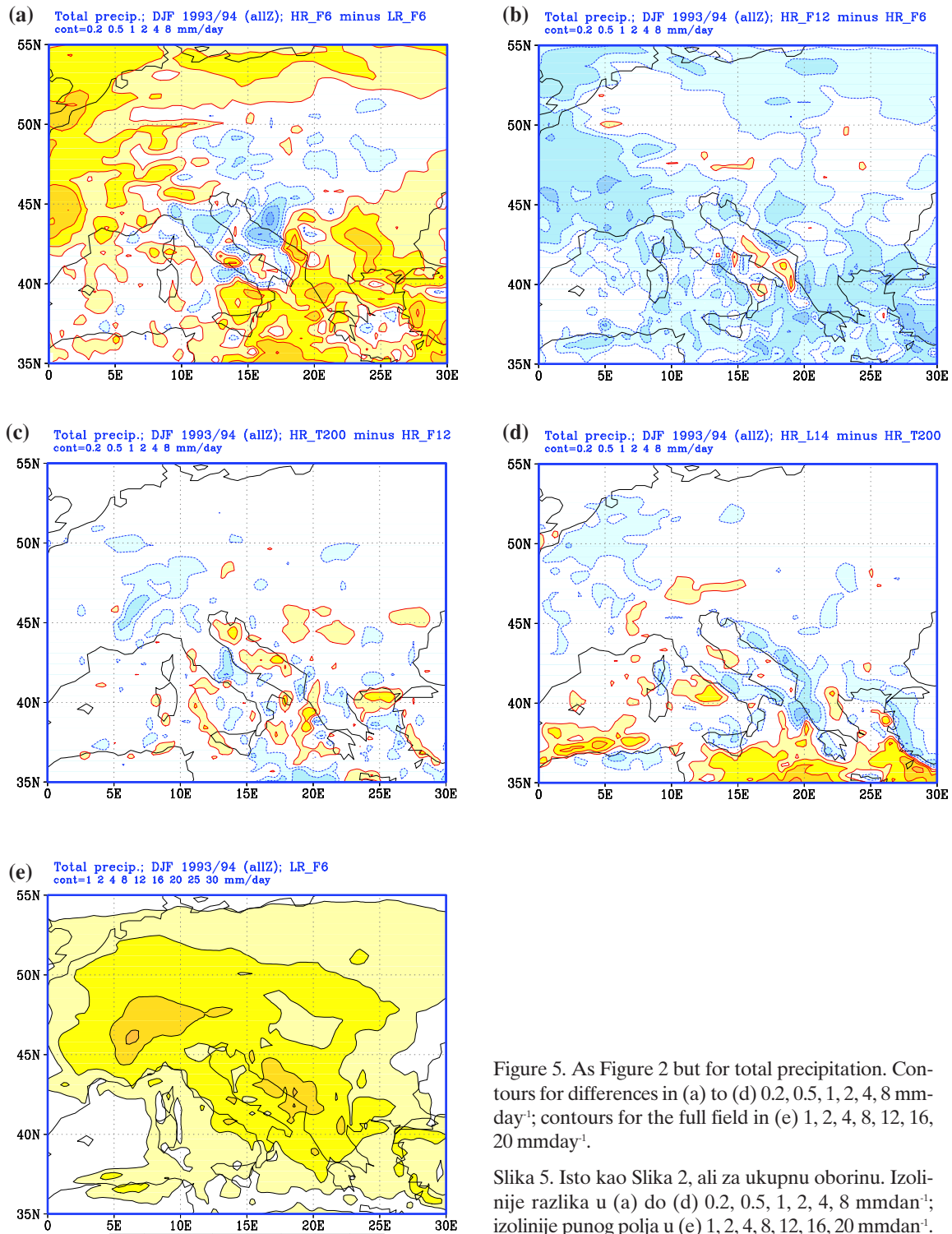
The DJF snow cover was found to be sensitive to changes in LBCs. The HR\_F6 minus LR\_F6 difference (Fig. 8 (a)) shows almost a continuous increase in snow cover over a wide area of central and eastern Europe. Only in small, isolated areas snow cover is smaller in HR\_F6 relative to LR\_F6. The largest increase is related to high mountains, reaching in places over 20 mm of water equivalent. This snow cover increase can be associated with the reduced surface temperature shown in Figure 7(a).

### 3.3. Impact of reduced LBCs frequency

As discussed earlier, the reduction in updating LBCs from 6-hour to 12-hour intervals may have a deteriorating effect on the processes that include the diurnal cycle. However, for many upper-air fields, the diurnal cycle is much reduced or almost non-existent when compared to their surface or near-surface counterparts. Nevertheless, the impact of the reduced frequency update of LBCs on 500 hPa geopotential height is rather striking. Figure 2 (b) clearly indicates an increase in heights in the winter season. The Mediterranean and southern Europe are more affected with this change than the northern part of the integration domain. Similar is the case in JJA (not shown); however, the JJA HR\_F12 minus HR\_F6 differences are halved when compared with those in DJF.

Predominantly positive differences in geopotential heights are also seen in vertical cross sections (Fig. 3 (b) and (d)), though in summer they are gradually reduced and become negative in the lower troposphere and close to the surface. The increase in the DJF geopotential height seen in Figure 3 (b) is only partly associated with an increase in temperature and this is confined mainly to the region close to the southern boundary (not shown). In JJA, the HR\_F12 temperature is higher than in HR\_F6 in almost the whole domain of the cross-section, even where the height differences in Figure 3(d) are negative.

Figures 2(b) and 3 (b) and (d) are based on the averages over all four post-processing times (00, 06, 12 and 18Z). However, when broken



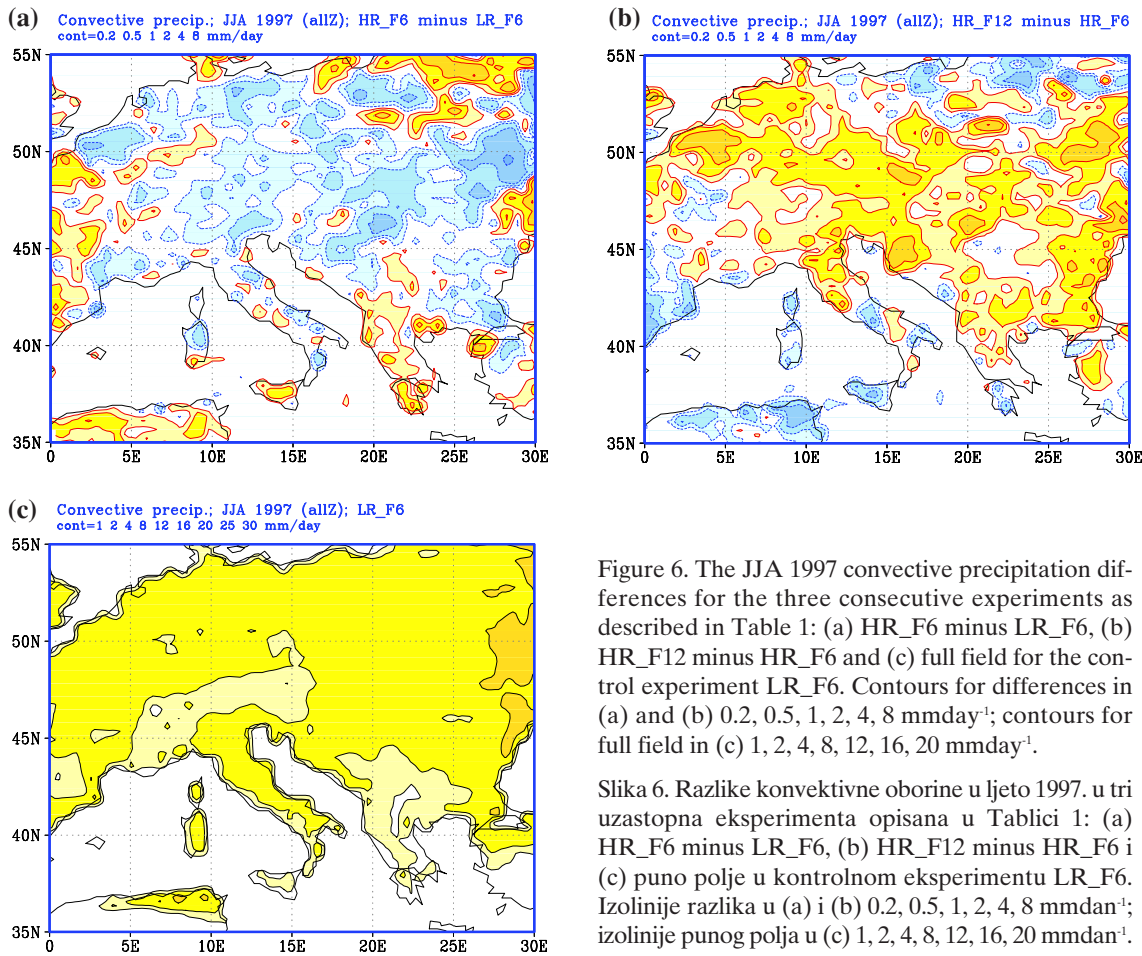


Figure 6. The JJA 1997 convective precipitation differences for the three consecutive experiments as described in Table 1: (a) HR\_F6 minus LR\_F6, (b) HR\_F12 minus HR\_F6 and (c) full field for the control experiment LR\_F6. Contours for differences in (a) and (b) 0.2, 0.5, 1, 2, 4, 8  $\text{mm day}^{-1}$ ; contours for full field in (c) 1, 2, 4, 8, 12, 16, 20  $\text{mm day}^{-1}$ .

Slika 6. Razlike konvektivne oborine u ljeto 1997. u tri uzastopna eksperimenta opisana u Tablici 1: (a) HR\_F6 minus LR\_F6, (b) HR\_F12 minus HR\_F6 i (c) puno polje u kontrolnom eksperimentu LR\_F6. Izolinije razlika u (a) i (b) 0.2, 0.5, 1, 2, 4, 8  $\text{mmdan}^{-1}$ ; izolinije punog polja u (c) 1, 2, 4, 8, 12, 16, 20  $\text{mmdan}^{-1}$ .

into individual times, the largest contribution to the pronounced positive height differences between HR\_F12 and HR\_F6 comes primarily from 06Z and 18Z. Thus, for example, in the southern half of the integration domain, positive differences at 06Z and 18Z exceed 2 dam and 1.6 dam respectively, whereas at 00Z and 12Z they are only around 0.5 dam with negative differences in the north (not shown). A reduced availability of some pieces of information in the HR\_F12 experiment makes a clear impact on height differences.

When averaged over the whole DJF season, the HR\_F6 geopotential height at 06Z is lower than that at 00Z, at 12Z it is higher than at 06Z, at 18Z it is again lower than at 12Z, and at 00Z it is higher than at 18Z. Thus, a reduction in geopotential height at 06Z and 18Z makes the HR\_F6 seasonal mean (averaged over all post-processing times) somewhat lower when compared to HR\_F12, where only data from 00Z and 12Z were used. This distinct

“oscillating” pattern seen in HR\_F6 can be traced back to the input ERA-40 data. Part of the answer to such behaviour lies with the ECMWF three-dimensional variational (3D-Var) data assimilation procedure that was used to generate the ERA-40 data. It may not be unlikely that observational data sources used for 06Z and 18Z were (systematically) different from those used for 00Z and 12Z. Namely, this discrepancy may be due to temperature biases in the satellite data relative to the radiosondes. At 06Z and 18Z, the analysis is strongly controlled by the satellite data which “move” the analysis one way; at 00Z and 12Z it is moved back by the radiosondes (Adrian Simmons, ECMWF, personal communication). In the current ECMWF operational analysis this oscillation is not seen because data assimilation is based upon the 4D-Var 12-hourly cycling.

From Figures 5 (b) through 8 (b) the impact of the reduced frequency in LBCs on some sur-

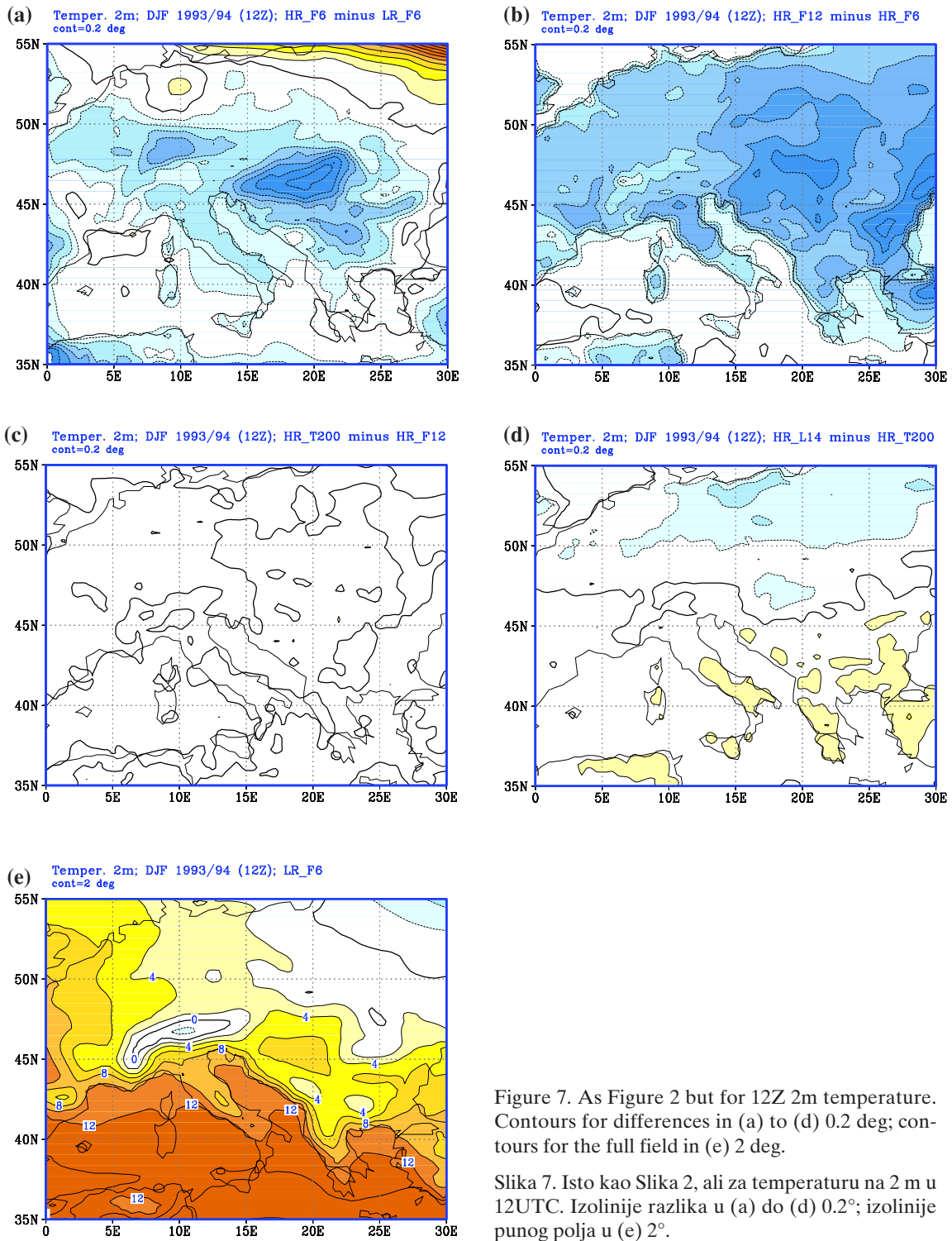


Figure 7. As Figure 2 but for 12Z 2m temperature. Contours for differences in (a) to (d) 0.2 deg; contours for the full field in (e) 2 deg.

Slika 7. Isto kao Slika 2, ali za temperaturu na 2 m u 12UTC. Izolinije razlika u (a) do (d) 0.2°; izolinije punog polja u (e) 2°.

face fields can be concluded. For precipitation, the overall impression is that the effect of the HR\_F12 minus HR\_F6 differences is the opposite to that of the HR\_F6 minus LR\_F6 differences. The reduced frequency of LBCs generally brings a reduction in total precipitation over most of Europe (mainly in the southern half), whereas the summer convective precipitation is increased (Fig. 5 (b) and 6 (b)). These changes slightly exceed  $1 \text{ mm day}^{-1}$ , similar to those in Figures 5 (a) and 6 (a). For the summer 2m temperature, the opposite effect to that for the previous change is also seen (not shown). It can be argued that for the above surface parameters a possible detrimental effect of the reduced frequency in LBCs cancels, to a certain degree, the (beneficial) effect of the increased resolution of LBCs.

For the DJF 2m temperature this, however, is not the case - it has been reduced further with the reduced frequency in LBCs (Fig. 7(b)). When compared with the Croatian observational data (see the preceding subsection) this seems to be beneficial. Consistent with this further cooling in the HR\_F12 experiment is an overall increase in snow cover (Fig. 8(b)). It is interesting to note that in some parts of the central and western Alps snow cover in HR\_F12 is actually reduced.

### 3.4. Impact of model changes in the vertical

In this subsection we consider both the impacts of the lowering of the model top level from 200 hPa to 100 hPa (HR\_T200 minus HR\_F12 in Table 1) and the reduction in the number of vertical levels when the top of the model is at 200 hPa (HR\_L14 minus HR\_T200). From Figure 2 (c) and (d) it can be concluded that the impact of these changes on the DJF 1993/94 500 hPa heights is insignificant in comparison to the impact of the changes discussed above. However, this is somewhat misleading because in the zonally averaged cross sections of geopotential heights the HR\_T200 minus HR\_F12 differences are relatively large with negative values above the 500 hPa level (not shown). The maximum difference, slightly above 1 dam, is found at the 200 hPa level in the southern part of the integration domain. The next modification – the reduction of model computational levels from 18 to 14 (HR\_L14 minus HR\_T200) – does not cause any substantial differences, as revealed by vertical cross sections.

The comparison of HR\_T200 minus HR\_F12 and HR\_L14 minus HR\_T200 was also possible for JJA 1997 through experiments with the Arakawa-Schubert closure (see Table 1). Whereas the reduced number of model levels brings, like in Figure 2 (d), negligible differences, the lowering of the model top causes negative differences of up to 0.5 dam over the south-eastern part of the integration domain (not shown). For the JJA HR\_T200 minus HR\_F12 cross section difference, a pattern similar to that in DJF emerges: relative large negative difference at the top of the model (over 1 dam) spreads deep down to the lower levels, almost reaching the surface.

In both the winter and summer seasons, the lowering of the model top causes a cooling of the upper troposphere (not shown), which is consistent with the negative differences in geopotential height described above. This cooling exceeds 1 deg in places over southeast Europe. When the number of vertical levels is reduced to 14, the temperature below 200 hPa is slightly increased, thus alleviating the cooling introduced with the changed top of the model.

In summer, both changes in the model vertical configuration affect the wind field: the lowering of the model top mostly influences upper-air wind; the reduction in model levels affects low-level wind. This is illustrated in Figure 9 for winds at 300 and 850 hPa levels. At 300 hPa, the westerlies over western and northern Europe prevail, whereas the northwesterlies in the northern Mediterranean are dominant (Fig. 9 (a)). These winds are a part of a much wider large-scale summer circulation that is characterised by an air flow directed from the summer Azores/European anticyclone towards the low pressure of the Indian monsoon. In the Mediterranean, the low-level northwesterly flow is known as the *etesian* wind (cf. Fig. 9(b)). Figure 9 (bottom panels) indicates that, in the Mediterranean region, both upper- and low-level winds are strengthened - aloft for more than  $1 \text{ ms}^{-1}$  and at 850 hPa level for nearly the same amount over the Tyrrhenian and Ionian Seas. At 850 hPa this makes a relative large increase, since low-level winds are much weaker than those at higher levels (cf. Figure 9(b)).

The impact of the changes in the model vertical configuration on some surface fields can be

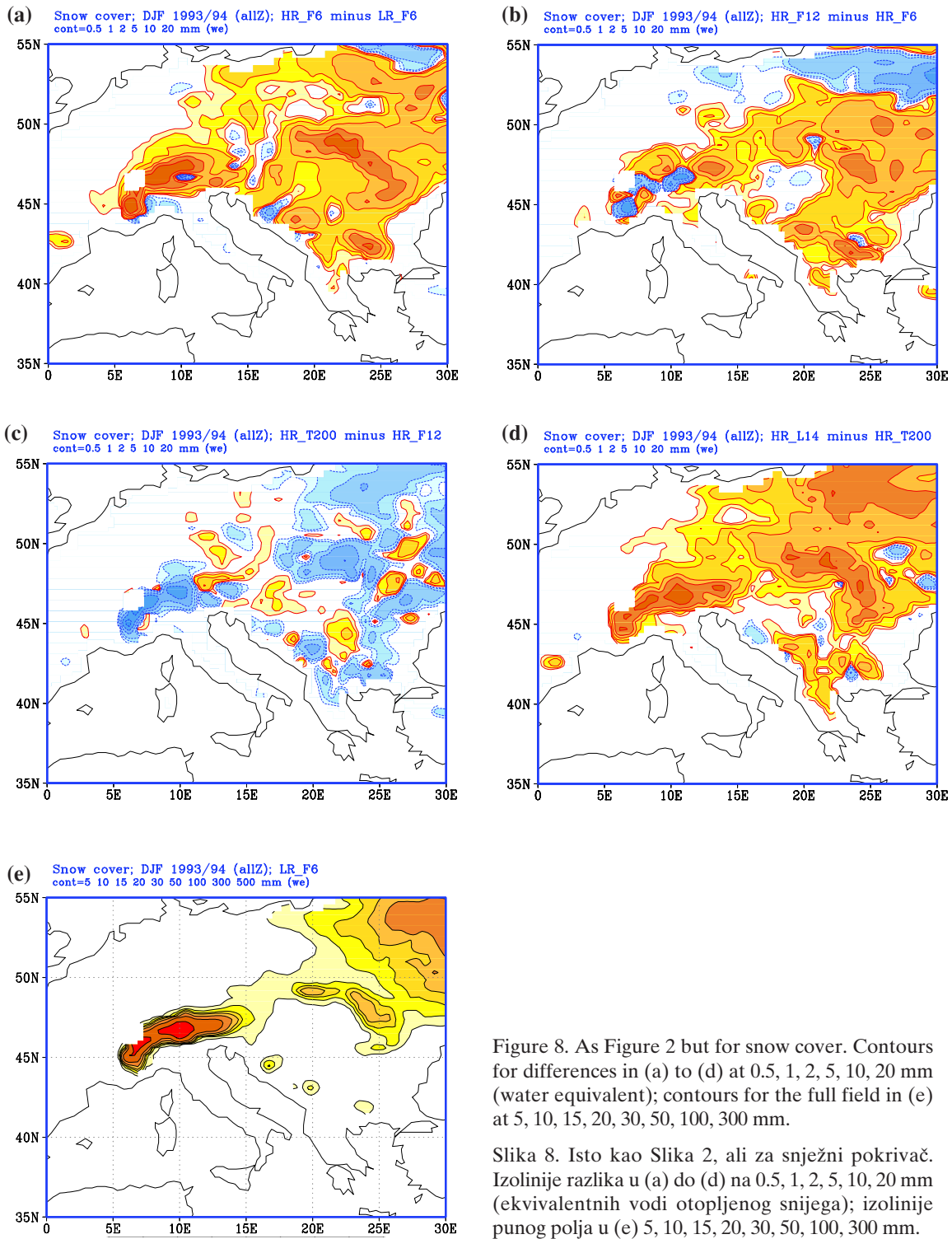


Figure 8. As Figure 2 but for snow cover. Contours for differences in (a) to (d) at 0.5, 1, 2, 5, 10, 20 mm (water equivalent); contours for the full field in (e) at 5, 10, 15, 20, 30, 50, 100, 300 mm.

Slika 8. Isto kao Slika 2, ali za snježni pokrivač. Izolinije razlika u (a) do (d) na 0.5, 1, 2, 5, 10, 20 mm (ekvivalentnih vodi otopljenog snijega); izolinije punog polja u (e) 5, 10, 15, 20, 30, 50, 100, 300 mm.

inferred from Figures 5, 7 and 8. For the DJF 1993/94, total precipitation and 2m temperature changes are much smaller than those related to the changes in LBCs. They are also of a rather small scale, patchy and incoherent. The only relatively large area of differences is seen over north Europe in Figure 7 (d).

A somewhat stronger signal is seen in snow cover (Fig. 8 (c) and (d)). The lowering of the model top generally causes an overall reduction in snow cover, though there are places where it was increased. Because there is al-

most no change in 2m temperature (Fig. 7(c)), it is not clear whether this tendency might be associated with a relative warming at the model's lowermost levels (not shown). With the reduced number of levels snow cover increases again over most of Europe (Fig. 8(d)).

In JJA, in the experiments with the Arakawa-Schubert closure (see Table 1), the reduction in the number of model levels has a larger impact on some surface fields than the lowering of the model upper boundary. Convective precipitation, more or less, uniformly increases

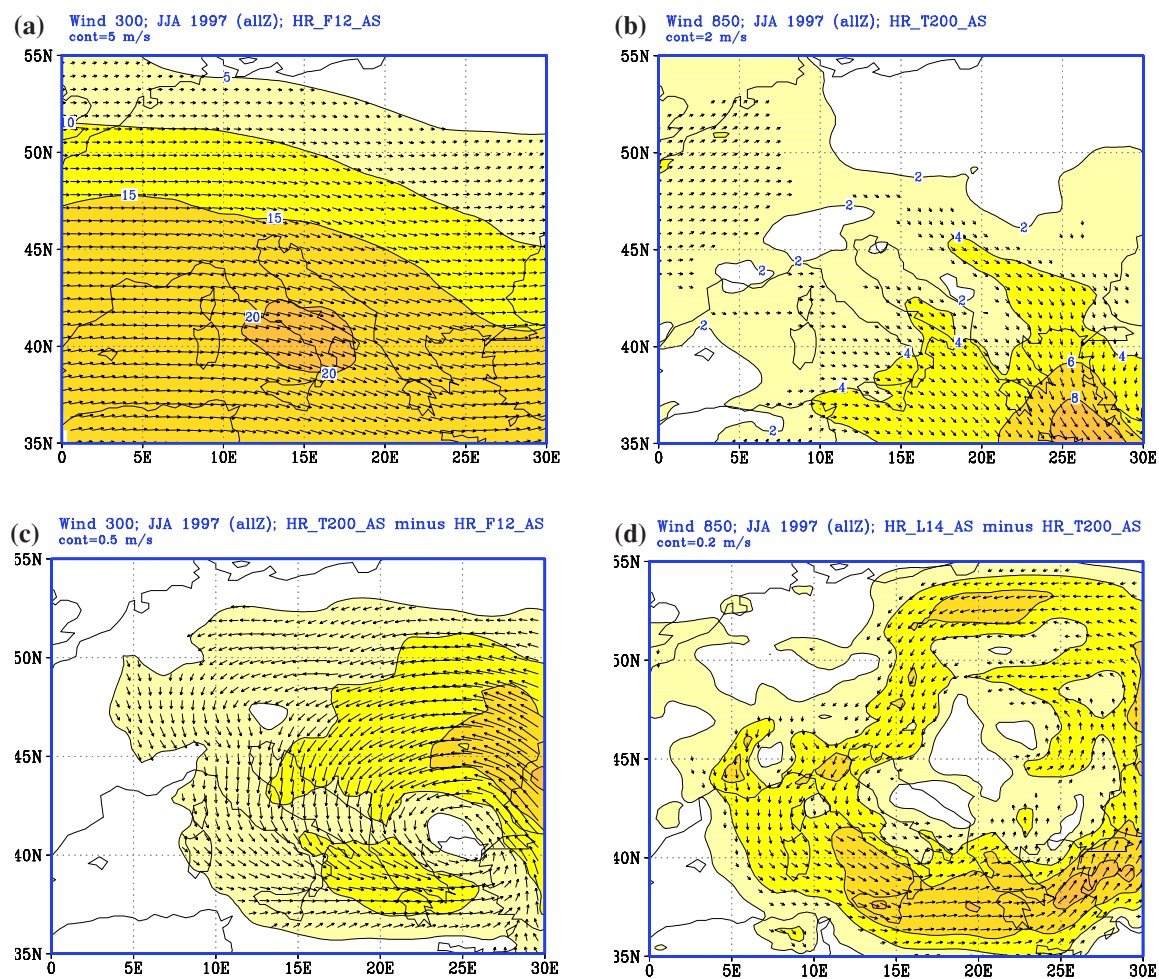


Figure 9. The JJA 1997 winds from experiments with the Arakawa-Schubert closure: for 300 hPa (left) and 850 hPa (right). The top panels are full fields: (a) HR\_F12, (b) HR\_T200. The bottom panels are the differences: (c) HR\_T200 minus HR\_F12 and (d) HR\_L14 minus HR\_T200. Contours every 5 and 2  $\text{ms}^{-1}$  for full fields and 0.5 and 0.2  $\text{ms}^{-1}$  for differences respectively.

Slika 9. Vjetar u ljeto 1997. u eksperimentima s Arakawa-Schubertovim zatvaranjem: na plohama 300 hPa (lijevo) i 850 hPa (desno). Gornje slike su puna polja: (a) HR\_F12, (b) HR\_T200. Donje slike jesu razlike: (c) HR\_T200 minus HR\_F12 i (d) HR\_L14 minus HR\_T200. Izolinije svakih 5 i 2  $\text{ms}^{-1}$  za puna polja odnosno 0.5 i 0.2  $\text{ms}^{-1}$  za razlike.

for about  $0.5 \text{ mm day}^{-1}$  all over continental Europe (not shown). This is associated with an increase in the daytime evapotranspiration, mostly for more than  $0.5 \text{ mm day}^{-1}$ . Over parts of western and central Europe this may be due to an increased near-surface mid-day temperature (not shown).

#### 4. IMPACT OF THE CHOICE OF CONVECTIVE SCHEME CLOSURE

It has been demonstrated in Section 3 that the RegCM response to imposed changes in LBCs was, on average, larger than that to changes in model vertical configuration. Therefore, additional experiments to test model sensitivity to the convective scheme closure were carried out for the summer HR\_F6 and HR\_F12 experiments. As mentioned in Section 2, two closures were considered: the Fritsch-Chappel closure (hereafter referred as to FC) and the Arakawa-Schubert closure (AS). Both closures were implemented in the RegCM as possible alternatives within the Grell convective precipitation scheme (Grell et al. 1994). The main difference between the two closures is in the definition of convective fluxes. Whereas the FC convective fluxes are based on the degree of instability in the atmosphere, the AS convective fluxes and precipitation are based on the tendencies in the state of the atmosphere. For both closures, the partitioning between convective and large-scale processes is based on their mutual statistical equilibrium.

From Figures 10 (c) and (d), a relative large reduction in convective precipitation in the AS with respect to the FC closure is seen in both HR\_F6 and HR\_F12. The reduction covers almost all continental Europe, but it is largest (between 2 and  $4 \text{ mm day}^{-1}$ ) in the flat lowlands of the western and central Europe and Russia. This indicates that, over a relatively flat underlying surface, the FC closure triggers convection (and consequently convective precipitation) far too often or for too long a period of time. This could be associated with the basic property of the FC closure - in summer, over continental regions, the atmosphere tends to be relatively unstable. Over the Alps, the difference in convective precipitation between the AS and FC closures is much reduced or almost zero, indicating that for high mountains both closure assumptions work in a similar way. The differences in convective pre-

cipitation full fields for the HR\_F12 experiments with the FC and AS closures can be also inferred from Figures 10 (a) and (b).

In contrast to convective precipitation, the differences in total precipitation over the Alps (and some other high grounds in the integration domain) are increased with the AS closure (Fig. 10 (e) and (f)). This points out that processes other than convection (e.g. large-scale condensation) produce more rain when this scheme is included in model physics. When compared with Croatia's observational data for JJA 1997, both closure assumptions yield reasonable good results for the continental part of the country; in the southern Adriatic, however, the AS closure is closer to reality - it tends to produce less total rainfall than the FC closure.

The reduction in convective precipitation in the AS closure compared to the FC is associated with a reduction in soil moisture, primarily over the model's low terrain (Fig. 11(c)). Over the Alps and other high mountains, soil moisture is increased with the AS, consistent with an overall increase in total precipitation. A drier soil over lowland Europe causes a warmer surface and near-surface temperature (Fig. 11 (a) and (b)). A warming in the 2m temperature is particularly strong during the night-time, amounting over 1 deg in parts of western and central Europe (Fig. 11(a)). This is primarily because there is almost no evaporation at night-time over the land surface (and consequently the night-time difference in evaporation between the AS and FC closures is essentially non-existent). The day-time evapotranspiration cools the 2m temperature (relative to its night-time values) and causes the 12Z AS minus FC temperature differences to be lower than those at 00Z (Fig. 11(b)). The difference in the mid-day evapotranspiration between the AS and FC closures is predominantly negative (Fig. 11(d)), again consistent with the reduction in convective (and total) precipitation and the reduction in soil moisture. The results for the HR\_F6 experiments are very similar to these above.

The changes in surface and near-surface temperature described above affect the upper-air fields, in particular those in the relative shallow layer of the lower troposphere. However, already at 850 hPa the sign of temperature dif-

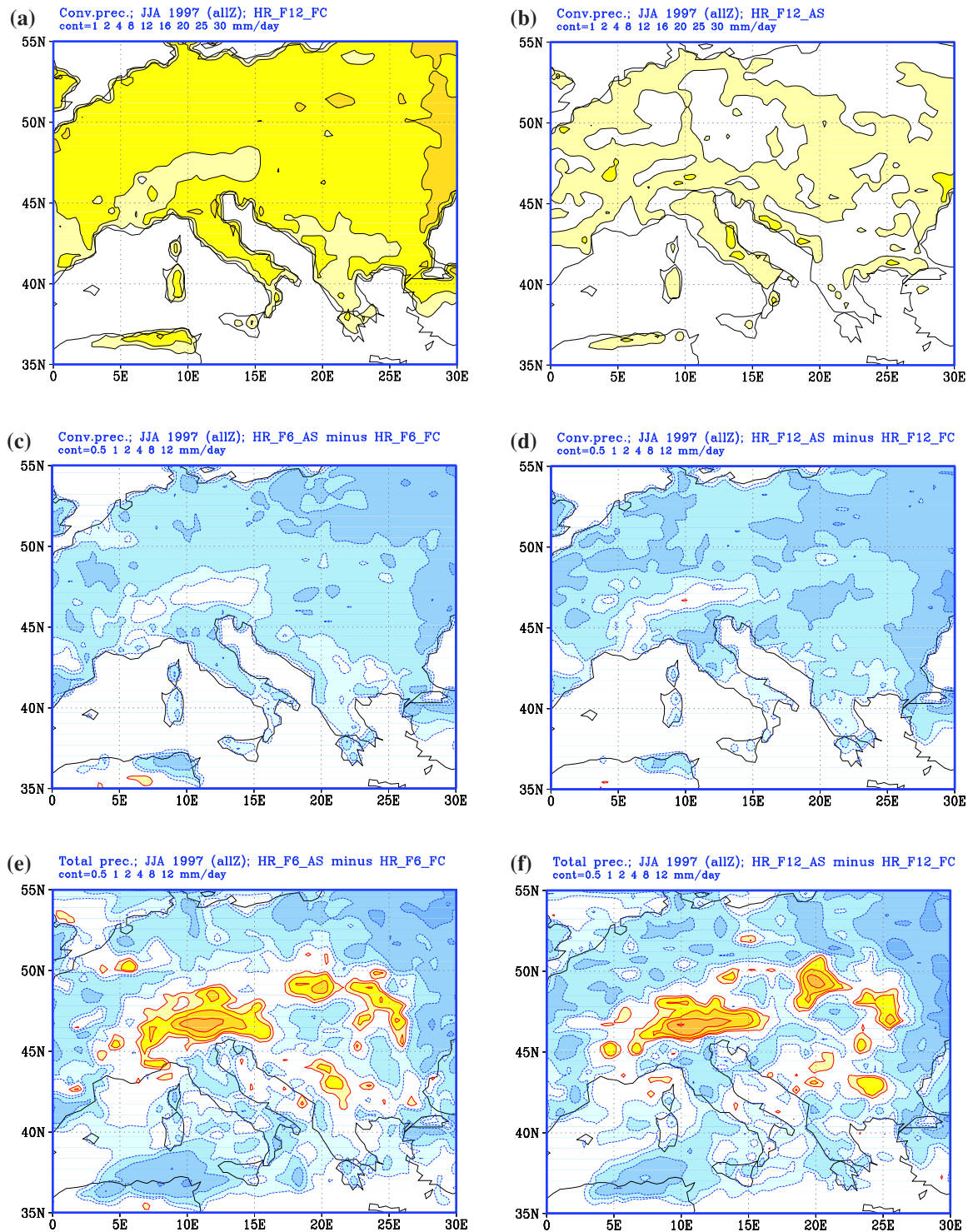


Figure 10. The JJA 1997 precipitation. Convective precipitation full fields for the HR\_F12 experiment for (a) with the FC closure and (b) with the AS closure. Convective precipitation differences AS minus FC for (c) HR\_F6 and (d) HR\_F12. Total precipitation differences AS minus FC for (e) HR\_F6 and (f) HR\_F12. Contours for full fields in (a) and (b) 1, 2, 4, 8, 12, 16, 20  $\text{mm day}^{-1}$ ; contours for differences in (c) to (f) 0.5, 1, 2, 4, 8  $\text{mm day}^{-1}$ .

Slika 10. Oborina u ljeto 1997. Puna polja konvektivne oborine u eksperimentu HR\_F12 s (a) FC zatvaranjem i (b) AS zatvaranjem. Razlike u konvektivnoj oborini između AS i FC zatvaranja u (c) HR\_F6 i (d) HR\_F12. Razlike u ukupnoj oborini između AS i FC zatvaranja u (e) HR\_F6 i (f) HR\_F12. Izolinije punog polja u (a) i (b) 1, 2, 4, 8, 12, 16, 20  $\text{mmdan}^{-1}$ ; izolinije razlika u (c) do (f) 0.5, 1, 2, 4, 8  $\text{mmdan}^{-1}$ .

ferences changes: positive differences are found only in the central part of the domain (mainly over higher topography) and negative ones in the outer areas. These affects, for example, the low-level circulation by weakening the etesian winds in the AS relative to the FC closure (not shown). The 200 hPa geopotential height difference between the AS and FC is all negative indicating a completely opposite effect when compared to the surface and near-surface temperature. For a better understanding of the processes involved in resulting in such a difference between the AS and FC clo-

tures, a detailed analysis of radiative processes, clouds as well as surface fluxes is required.

## 5. VERIFICATION OF MODEL RESULTS

Verification of model results makes an important part in the assessment of overall model performance. Here, only a brief discussion on verification of the selected model fields is given. The upper-air model data are verified against ERA-40, and for the verification of precipitation the dataset from the Climatic Research Unit (CRU) of the University of East Anglia

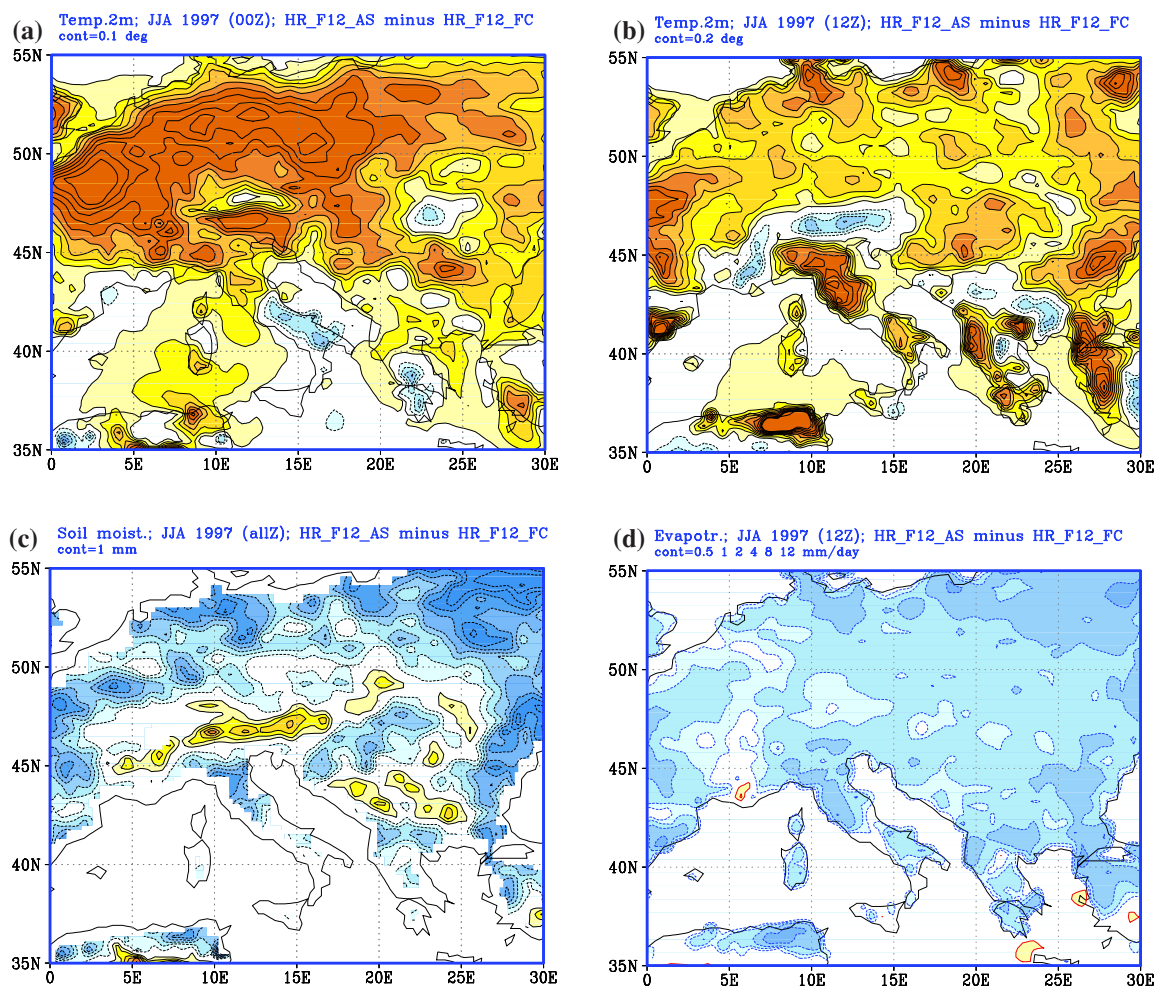


Figure 11. The JJA 1997 AS minus FC differences in some surface fields for the HR\_F12 configuration. Top: 2m temperature at (a) 00Z and (b) 12Z. Bottom: (c) soil moisture and (d) evapotranspiration at 12Z. Contours for temperature differences in (a) and (b) every 0.1 deg, for soil moisture differences in (c) 1 mm, and for evapotranspiration in (d) at 0.5, 1, 2, 4, 8, 12 mmday<sup>-1</sup>.

Slika 11. Razlike AS minus FC u nekim prizemnim poljima u ljeto 1997. za HR\_F12 konfiguraciju. Gore: temperatura na 2m u (a) 00UTC i (b) 12UTC. Dolje: (c) vlažnost tla i (d) evapotranspiracija u 12UTC. Izolinije za temperaturne razlike u (a) i (b) svakih 0.1°, za razlike u vlažnosti tla u (c) 1 mm i za evapotranspiraciju u (d) na 0.5, 1, 2, 4, 8, 12 mmdan<sup>-1</sup>.

was used (New et al., 1999, 2000). For upper-air fields both model and verifying data were interpolated to the 2x2 latitude/longitude grid; for precipitation, the CRU data were interpolated to the model grid.

In Figure 12, the verification results for the HR\_L14 experiments are only shown, because, as discussed in Section 2.2, the HR\_L14 configuration is closest to that in the ECMWF seasonal forecast archive. From Figure 12 (top and middle panels) it is clear that both model mid-troposphere geopotential height and low-troposphere temperature exhibit lower values when compared with ERA-40. The pattern of negative errors showed in Figure 12 is similar in both DJF 1993/94 and JJA 1997 with somewhat larger model errors in the JJA season. In particular, this is the case with the 850 hPa temperature, where the error amounts to more than -3 deg in the southeastern part of the integration domain. In winter, the temperature error over the same area is halved when compared to that in summer (cf. contouring intervals in Figures 12 (c) and (d)).

Though the HR\_L14 experiments represent the most "degraded" model and LBCs configuration, the errors shown in Figure 12 are not necessarily the largest. For example, for the winter 500 hPa heights the HR\_L14 errors are as large as in other HR experiments and in the LR\_F6 experiment the errors are the smallest (not shown). The same is true for the DJF 850 hPa temperature. On the other hand, the 850 hPa summer temperature errors are the smallest in all the HR\_F12 configurations (the last three listed in Table 1), while the HR\_F6 exhibits the largest errors. Irrespective of season, for both Z500 and T850, the error increases when the resolution is increased from T42 to T159. A possible explanation could be in the interpolation of the model and verifying fields to a 2x2 deg lat/lon grid which might favour a coarser, T42, resolution of the LR\_F6 LBCs.

In contrast to the lower troposphere temperature and geopotential errors, the 300 hPa temperature error pattern shows a different behaviour (Fig. 12 (e) and (f)). They are positive with similar amplitude in both seasons. The smallest errors are found for the HR\_T200 configuration with a slight increase in HR\_L14. The HR\_F6 errors are smaller than those in LR\_F6. No plausible explanation can

be offered for such a change of sign in temperature biases with height; however, Qian et al. (2003) found a similar warm bias of about 1 deg in the upper troposphere of their continuous RegCM2 simulation over tropical South America.

For precipitation, in DJF, positive errors prevail in the inner part of the integration domain, whilst negative errors are mainly located towards the domain edges (Fig. 13 (a)). In summer, positive errors are spread over almost the entire domain (Fig. 13 (b)). In both seasons, most of the precipitation errors can be associated with some orographic features (the Alps, the mountains of the Balkan Peninsula, the Carpathian Mountains); however, they are also found over relatively flat terrain. Relatively large errors in summer (between 2 and 4 mmday<sup>-1</sup>) may seem a serious drawback if one bears in mind the generally small precipitation amounts in this season; however, even larger summer precipitation errors (up to 18 mmday<sup>-1</sup>) were reported for a different regional model (Christensen et al., 2001). As mentioned earlier, a single model realisation is insufficient to draw any definite conclusion on the significance of this result.

The precipitation verification for the JJA HR\_F12 experiments with the two different closures (FC and AS, cf. Table 1) is shown in Figure 13 (c) and (d). Whereas for the FC closure the negative errors in the central part of the integration domain could be associated with some mountain ranges, the positive errors largely correspond to lowland regions (western and northern Europe, Hungarian plain, Russia). It is likely that some positive errors in the FC closure are caused by an overestimated summer convective rainfall as indicated in Figure 10 (a). With the AS closure these positive errors are reversed, i.e. they became negative (Fig. 13 (d)). Again, this may be linked to a largely reduced convective precipitation with the AS scheme as shown in Figure 10 (b). The negative errors in both FC and AS closures associated with mountain ranges may indicate a too low orography used in our model integrations.

## 6. SUMMARY AND CONCLUSIONS

A series of seasonal dynamical downscaling experiments with the Regional Climate Model (RegCM) has been conducted in order to as-

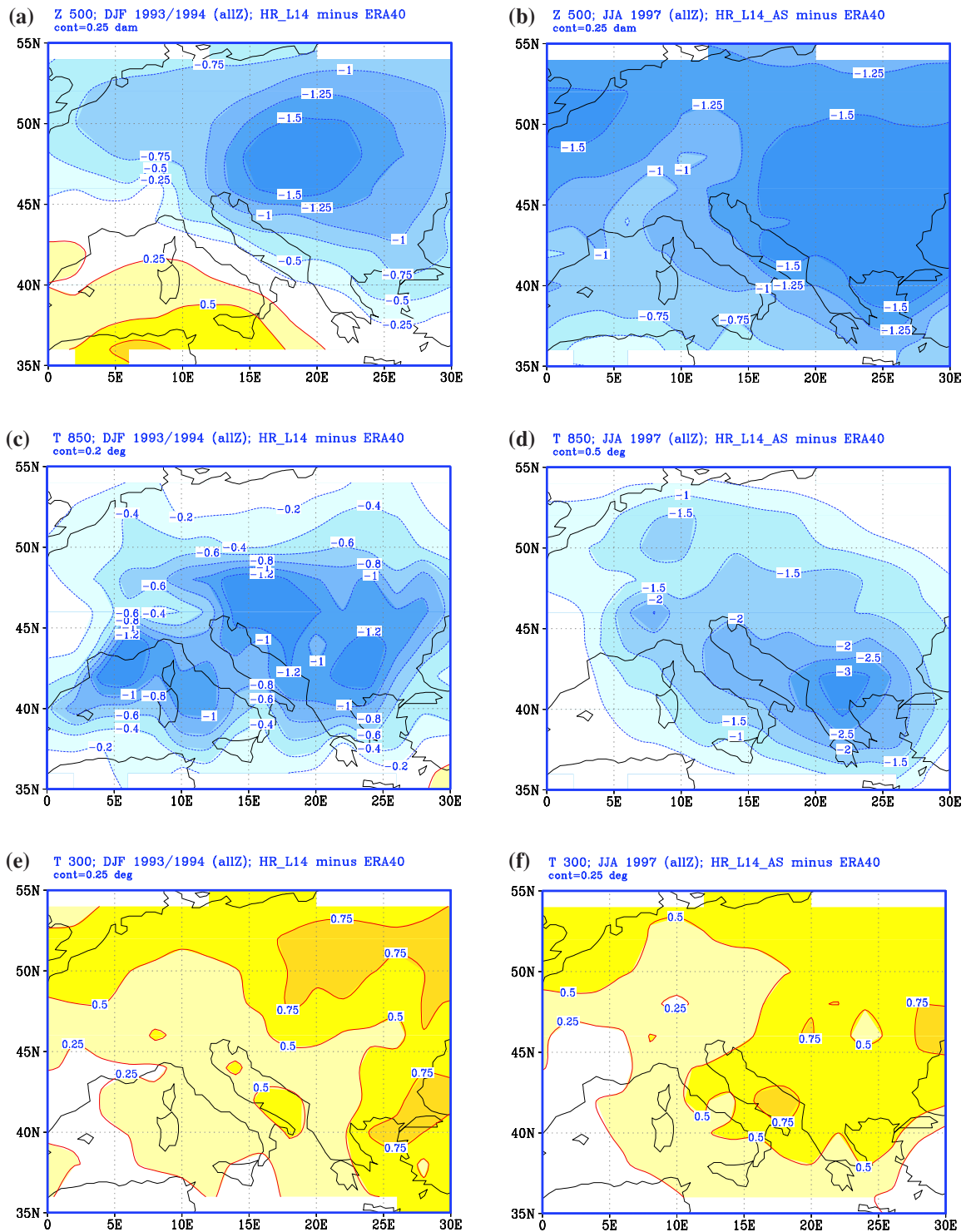


Figure 12. Verification of the RegCM HR\_L14 experiments for DJF 1993/94 (left) and JJA 1997 (right): for 500 hPa geopotential height (top), 850 hPa temperature (middle) and for 300 hPa temperature (bottom). Contours for geopotential every 0.25 dam, for 850 hPa temperature 0.2 and 0.5 deg, and for 300 hPa temperature 0.25 deg.

Slika 12. Verifikacija RegCM HR\_L14 eksperimenata za zimu 1993/94. (lijevo) i ljeto 1997. (desno): geopotencijal plohe 500 hPa (gore), temperatura na 850 hPa (sredina) i temperatura na 300 hPa (dolje). Izolinije za geopotencijal svakih 0.25 dam, za temperaturu na 850 hPa 0.2° i 0.5° i za temperaturu na 300 hPa 0.25°.

sess the model sensitivity to changing initial conditions (ICs), lateral boundary conditions (LBCs) and the model vertical configuration. The ICs and LBCs were taken from the ECMWF re-analysis archive (ERA-40).

The model response was first tested to the increased resolution in the ICs and LBCs from T42 to T159. Then the experiments were designed in such a way as to test model sensitivity to the loss of information at the LBCs and in the vertical when approaching as close as possible to the temporal and spatial resolutions of the data available from the ECMWF seasonal forecasts archive. Therefore, the frequency of the LBCs update was reduced from

6-hourly to 12-hourly intervals, the model upper boundary (top of the model) was lowered from 100 hPa to 200 hPa and, finally, the number of model levels in the vertical was reduced from 18 to 14. The experiments were carried out for two different seasons: one winter, DJF 1993/94 and one summer, JJA 1997.

The RegCM was integrated over the central European and the northern Mediterranean domain centred at a point in Croatia: 45°N and 16°E. The model resolution was 50 km, with 60 and 50 points in the longitudinal and latitudinal directions respectively, thus making a domain size of approximately 3000x2500 km. All winter integrations were made with the

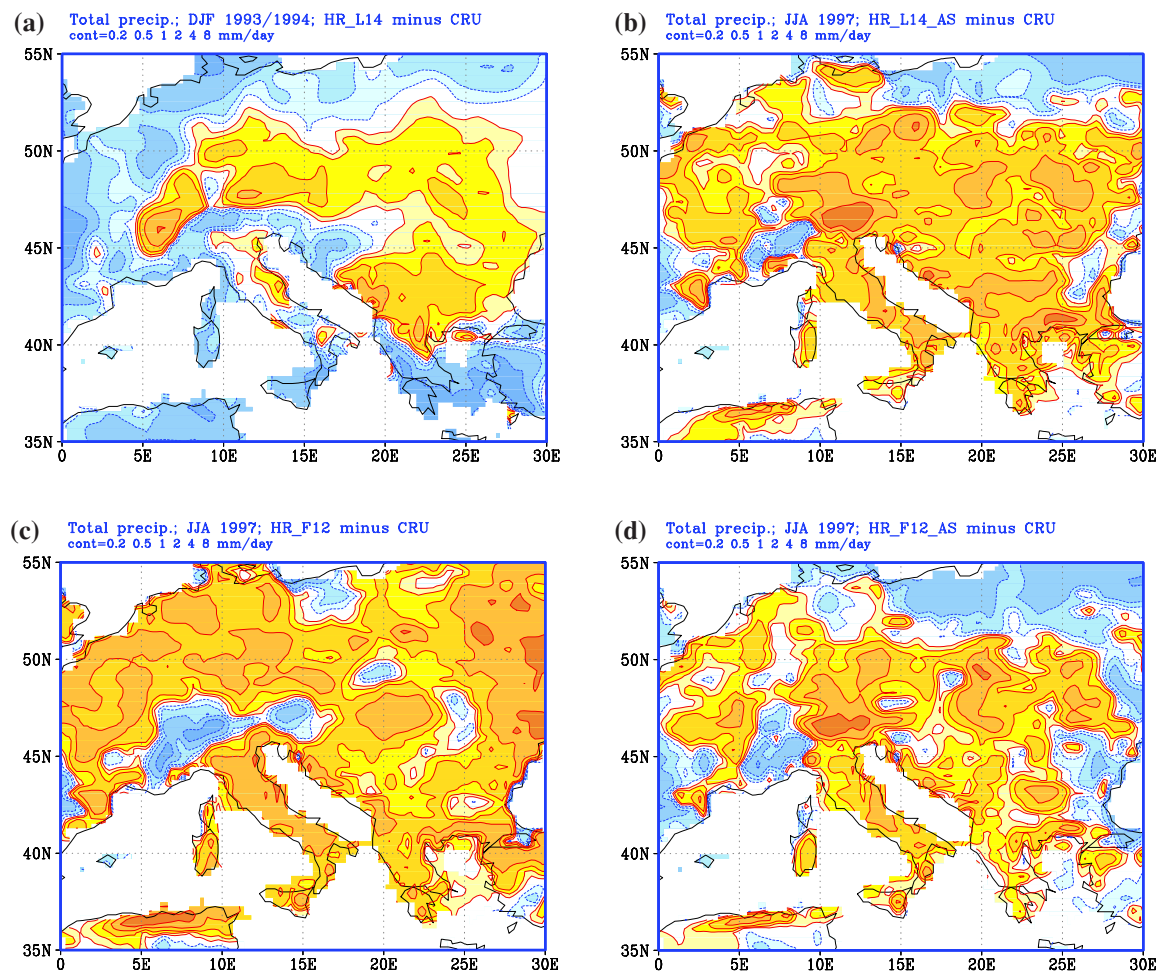


Figure 13. Verification of total precipitation for the model HR\_L14 experiments (top) for: (a) DJF 1993/94 and (b) JJA 1997. Verification for the JJA 1997 HR\_F12 experiments (bottom) for: (c) Fritsch-Chappel closure and (d) Arakawa-Schubert closure. Contours at 0.2, 0.5, 1, 2, 4, 8 mmday<sup>-1</sup>.

Slika 13. Verifikacija ukupne oborine u eksperimentima HR\_L14 (gore) (a) za zimu 1993/94. i (b) za ljeto 1997. Verifikacija eksperimenata HR\_F12 u ljeto 1997. (dolje): (c) za Fritsch-Chappelovo zatvaranje i (d) Arakawa-Schubertovo zatvaranje. Izolinije na 0.2, 0.5, 1, 2, 4, 8 mmdan<sup>-1</sup>.

Fritsch-Chappel closure in the parameterization of convection. In summer, for some LBCs and model configurations, additional integrations with the Arakawa-Schubert convection closure were carried out. This made it possible to test model sensitivity to different closures during the period with increased convective activity.

Of course, the forcings from these various external (LBCs) and internal (the vertical domain) configurations have yielded different model responses. However, it is important to stress that most differences in the model response are comparably small, though by no means negligible. In most cases they do not significantly alter the meteorological significance of the fields considered. Qian et al. (2003) also found that model simulations are more similar to each other than to the reanalysis, though the experimental design in their study differs from the one discussed here. However, local differences in model results may have an impact on the model local mean and seasonal climate variability. In particular, this is the case for the details in the fields' structure related to and dependent on the representation of orography.

Some of the model responses can be summarised as follows: the increase in the resolution of the ICs and LBCs from T42 to T159 (whilst retaining the frequency of the LBCs update) causes, on average, a general reduction in geopotential heights and temperature (cooling). In winter, this cooling is more pronounced in the lower troposphere, whilst in summer, the cooling is stronger in the upper troposphere and lower stratosphere. This upper atmospheric cooling has its near-surface counterpart – the 2m temperature in both seasons is cooler with T159 than with T42 LBCs and it is larger in DJF than in JJA. The DJF near-surface cooling may have an impact on snow cover, which is increased with a higher resolution (T159) of the LBCs. Though, in both seasons, the total precipitation response is not unique, a clear signal emerges in summer convective precipitation – it is reduced in almost the entire integration domain with the T159 LBCs.

The impact of the reduced frequency update in LBCs from 6-hourly to 12-hourly intervals on most upper-air fields is of the opposite sign to that seen when the LBCs resolution is in-

creased from T42 to T159. It mostly brings an increase in geopotential heights and temperature (warming). However, it is argued that such a model response is primarily driven by a particular feature in the ERA-40 upper-air data: they tend to “oscillate” between consecutive 6 hours because of the difference in the processing of the temperature field between the satellite and radiosonde data. When the 12-hourly sampling for LBC is applied, this “oscillation” is lost. Therefore, it was not possible to fully establish to what extent the reduction from 6-hourly to 12-hourly LBCs frequency has a detrimental effect on model integrations.

Similar to upper-air fields, the impact of the reduced LBCs frequency on many surface and near-surface fields is to counteract the effects of increased resolution. For example, whilst the winter total precipitation is generally reduced, the summer convective precipitation is increased. It can be argued therefore that, for some surface parameters, a possible detrimental effect of the LBCs frequency reduction cancels, to a certain degree, a possibly beneficial effect of the increased resolution in LBCs. On the other hand, the reduction in the LBCs frequency causes the winter 2m temperature to further cool, thus resulting in a further increase in snow cover.

The lowering of the model top from 100 to 200 hPa causes in both seasons a reduction (cooling) in the upper model atmosphere geopotential heights (temperature). In summer, this effect is extended into the middle and lower model troposphere. It causes a strengthening of the upper troposphere northwesterly winds over south Europe and the northern Mediterranean. The reduction of model levels from 18 to 14 alleviates somewhat the effects of the lowering of the model upper boundary. However, it also causes an increase in the low-level summer etesian wind. For many surface fields, the impact of changes in the model vertical configuration is generally weaker than the impact of the changes in LBCs. The most notable exception is a somewhat larger increase in the summer convective rainfall, evapotranspiration and 2m temperature.

The main difference between the Arakawa-Schubert (AS) and Fritsch-Chappel (FC) closures tested in the summer integrations is a reduced amount of convective precipitation over the north European lowlands in the former

with respect to the latter. The reduced rainfall is associated with a reduced amount of water available to penetrate into the soil and for evapotranspiration. This in turn makes the near-surface temperature increase over many parts of Europe in the integrations with the AS closure.

A limited verification of model results gives an indication of the model overall performance. It was found that, for selected LBCs and model configuration (high resolution, 12-hourly updates with model top at 200 hPa) and irrespective of season, the model underestimates geopotential heights and low-level temperature, but overestimates temperature at upper levels. The precipitation is overestimated over the central and southern parts of the integration domain (mainly over the mountains).

The first experience with the RegCM in the CMHS is certainly encouraging and further testing and assessment of model integrations will be continued. It has been demonstrated that the loss of information in the ICs and LBCs as well as the “deterioration” in the model vertical configuration do not affect seasonal downscaling so as to make it unviable. The next step, a continuation of the experiments described and discussed here, will be with ECMWF seasonal ensemble forecasts. Assuming that the differences between ensemble members might be taken as typical of perturbations in ICs and LBCs, they will also make possible to address the question of the model internal variability. The results of such a project will be reported in due course.

**Acknowledgement:** We thank Xungqiang Bi and Jeremy Pal from the Physics of Weather and Climate Group of the Abdus Salam International Centre for Theoretical Physics in Trieste, Italy, for their help in installing and setting up the RegCM in CMHS. We also thank Filippo Giorgi for his valuable comments and suggestions that improved the quality of this paper.

## REFERENCES

- Anthes, R., 1977: A cumulus parameterization scheme utilizing a one-dimensional cloud model. *Mon. Wea. Rev.*, **117**, 1423–1438.
- Arakawa, A. and W.H. Schubert, 1974: Interaction of a cumulus cloud ensemble with the large scale environment, Part I. *J. Atmos. Sci.*, **31**, 674–701.
- Betts, A.K. and M. Miller, 1993: The Betts-Miller scheme. Chapter 9 in: *The representation of cumulus convection in numerical models of the atmosphere* (Eds. K.A. Emanuel and D.J. Raymond). *Meteo. Mon. Amer. Met. Soc.*, 107–121.
- Christensen, O.B., M.A. Gaertner, J.A. Prego and J. Polcher, 2001: Internal variability of regional climate models. *Clim. Dyn.*, **17**, 875–887.
- Dickinson, R.E., R.M. Errico, F. Giorgi and G.T. Bates, 1989: A regional climate model for the western United States. *Clim. Change*, **15**, 383–422.
- Dickinson, R.E., A. Henderson-Sellers and P.J. Kennedy, 1993: Biosphere-atmosphere transfer scheme (BATS) version 1e as coupled to the NCAR Community Climate Model, *NCAR Tech. Note NCAR/TN-387+STR*, NCAR, Boulder, Colorado, USA, 80 pp.
- Fritsch, J.M. and C.F. Chappell, 1980: Numerical prediction of convectively driven mesoscale pressure systems. Part I: Convective parameterization. *J. Atmos. Sci.*, **37**, 1722–1733.
- Giorgi, F., 1990: Simulation of regional climate using a limited area model nested in a general circulation model. *J. Climate*, **3**, 941–963.
- Giorgi, F., X. Bi and J.S. Pal, 2004: Mean, interannual variability and trends in a regional climate change experiment over Europe. I. Present-day climate (1961–1990). *Clim. Dyn.*, **22**, 733–756.
- Giorgi, F., M.R. Marinucci and G.T. Bates, 1993a: Development of a second-generation regional climate model (RegCM2), Part I: Boundary-layer and radiative transfer processes. *Mon. Wea. Rev.*, **121**, 2794–2813.
- Giorgi, F., G. De Canio and G.T. Bates, 1993b: Development of a second-generation regional climate model (RegCM2), Part II: Convective processes and assimilation of lateral boundary conditions. *Mon. Wea. Rev.*, **121**, 2814–2832.
- Giorgi, F. and L.O. Mearns, 1999: Introduction to special section: Regional climate modeling revisited. *J. Geophys. Res.*, **104**, D6, 6335–6352.

- Grell, G.A., 1993: Prognostic evaluation of assumptions used by cumulus parameterizations. *Mon. Wea. Rev.*, **121**, 764–787.
- Grell, G.A., J. Dudhia and D.R. Stauffer, 1994: A description of the fifth-generation Penn State/NCAR mesoscale model (MM5). *NCAR Tech. Note TN-398+IA*. NCAR, Boulder, Colorado, USA, 125 pp.
- Holtslag, A.A.M., E.I.F. de Bruijn and H.L. Pan, 1990: A high resolution air mass transformation model for short-range weather forecasting. *Mon. Wea. Rev.*, **118**, 1561–1575.
- Kiehl, J., J. Hack, G. Bonan, B. Boville, B. Breigleb, D. Williamson and P. Rasch, 1996: Description of the NCAR Community Climate Model (CCM3), *NCAR Tech. Note NCAR/TN-420+STR*. NCAR, Boulder, Colorado, USA, 160 pp.
- New, M.G., M. Hulme and P.D. Jones 1999: Representing twentieth-century space time climate variability. Part I. Development of the 1961–1990 mean monthly terrestrial climatology. *J. Clim.*, **12**, 829–856.
- New, M.G., M. Hulme and P.D. Jones 2000: Representing twentieth-century space time climate variability. Part II. Development of the 1901–1996 mean monthly terrestrial climatology. *J. Clim.*, **13**, 2217–2238.
- Pal, J.S., E.E. Small and E.A.B. Elthair, 2000: Simulation of regional-scale water and energy budgets: Representation of subgrid cloud and precipitation processes within RegCM. *J. Geophys. Res.*, **105**, 29579–29594.
- Pan, Z., E. Takle, W. Gutowski and R. Turner, 1999: Long simulation of regional climate as a sequence of short segments. *Mon. Wea. Rev.*, **127**, 308–321.
- Qian, J-H., A. Seth and S. Zebiak, 2003: Reinitialized versus continuous simulations for regional climate downscaling. *Mon. Wea. Rev.*, **131**, 2857–2874.
- Wilby, R.L. and T.M.L. Wigley, 1997: Downscaling general circulation model output: a review of methods and limitations. *Prog. Phys. Geogr.*, **21**, 530–548.
- Zeng, X. and R.A. Pielke, 1995: Landscape-induced atmospheric flow and its parameterization in large-scale numerical models. *J. Clim.*, **8**, 1156–1177.
- Zeng, X., M. Zhao and R.E. Dickinson, 1998: Intercomparison of bulk aerodynamic algorithms for the computation of sea surface fluxes using the TOGA COARE and TAO data. *J. Clim.*, **11**, 2628–2644.